SCIENCE CHINA
Earth Sciences

SPECIAL TOPIC: Destruction of craton and subduction of western Pacific plate
•REVIEW•

June 2018 Vol.61 No.6: 711–729
https://doi.org/10.1007/s11430-017-9185-2

# Carbonate metasomatism in the lithospheric mantle: Implications for cratonic destruction in North China

Keqing ZONG* & Yongsheng LIU

*State Key Laboratory of Geological Processes and Mineral Resources; School of Earth Sciences, China University of Geosciences, Wuhan 430074, China*

Received June 30, 2017; revised February 24, 2018; accepted March 7, 2018; published online April 12, 2018

**Abstract** The activity of melts and fluids may have played a key role in inducing the destruction of the eastern North China Craton in the early Cretaceous. Carbonate melts are important agents in mantle metasomatism and can significantly modify the physical and chemical properties of the subcontinental lithospheric mantle. Carbonate metasomatism can be identified by specific geochemical indices in clinopyroxene, such as high Ca/Al and low Ti/Eu ratios. This study presents the spatial and temporal variations of carbonate metasomatism in the lithospheric mantle beneath the eastern North China Craton. Three types of carbonate metasomatism are classified based on the geochemical compositions of clinopyroxene in mantle peridotites. Clinopyroxene formed by Type 1 carbonate metasomatism is characterized by very high Ca/Al ratios (15–70) and $^{87}Sr/^{86}Sr$ ratios (0.706–0.713). Clinopyroxene derived from Type 2 carbonate metasomatism shows relatively high Ca/Al ratios (5–18) and $^{87}Sr/^{86}Sr$ ratios (0.703–0.706). However, clinopyroxene resulting from Type 3 carbonate metasomatism has low Ca/Al ratios (5–9) and $^{87}Sr/^{86}Sr$ ratios (0.702–0.704). Deep (garnet-bearing) and shallow (spinel-bearing) lithospheric mantle beneath the Sulu orogen and surrounding areas in the eastern North China Craton were affected by intense Type 1 carbonate metasomatism before the late Triassic. The deep subduction of the South China Block with its accompanying carbonate sediments was the trigger for Type 1 carbonate metasomatism, which reduced strength of the lithospheric mantle and provided a prerequisite for the destruction of the eastern North China Craton in the early Cretaceous. After the destruction of the eastern North China Craton, the ancient relict lithospheric mantle, represented by spinel harzburgite xenoliths hosted in the late Cretaceous to Cenozoic basalts, only recorded Type 2 carbonate metasomatism. This implies that the lithospheric mantle experienced the intense Type 1 carbonate metasomatism was completely destroyed and not preserved during decratonization. Spinel lherzolite xenoliths hosted in the late Cretaceous to Cenozoic basalts represent the young, fertile lithospheric mantle formed after the cratonic destruction and only a few samples record Type 2 and 3 carbonate metasomatisms. We suggest that carbonate melts derived from the subduction-modified asthenospheric mantle with variable proportions of recycled crustal material was responsible for the Type 2 and 3 carbonate metasomatisms. The carbonate metasomatism of the lithospheric mantle beneath the Jiaodong Peninsula and surrounding areas is very pervasive and is spatially consistent with the remarkable thinning of lithospheric mantle and giant gold deposits in this region. Therefore, we conclude that carbonate metasomatism in the lithospheric mantle played a crucial part in the modification, destruction and gold deposits in the eastern North China Craton.

**Keywords** Cratonic destruction, North China, Carbonate metasomatism, Ca/Al in clinopyroxene, Lithospheric mantle

**Citation:** Zong K, Liu Y. 2018. Carbonate metasomatism in the lithospheric mantle: Implications for cratonic destruction in North China. Science China Earth Sciences, 61: 711–729, https://doi.org/10.1007/s11430-017-9185-2

* Corresponding author (email: kqzong@hotmail.com)

## 1. Introduction

Archean cratons generally have thick (>200 km) lithospheric mantle keels and are characterized by low densities and low surface heat flows. They are considered to be the most stable regions on Earth and have low levels of tectonism, magmatism, mineralization and earthquakes (Sleep, 2003; Carlson et al., 2005; Lee et al., 2011). The North China Craton has some characteristics in common with other Archean cratons, such as the preservation of ancient crustal remnants as old as 3.8 Ga (Liu et al., 1992), a stable environment from 1.9–1.8 Ga to the Paleozoic (Zhao et al., 2001; Zhao and Zhai, 2013) and a thick lithospheric mantle keel (Gao et al, 2002; Zhang H F et al., 2008). However, in contrast to other Archean cratons, the North China Craton experienced intense reactiviation and modification in the Mesozoic (Chen, 1956; Zhang et al., 2003; Gao et al., 2004; Wu et al., 2005)—as shown by widespread structural deformation, magmatism, the presence of fault-bounded basins and mineralization (Li et al., 2012; Meng, 2003; Zhu G et al., 2012, 2015; Deng and Wang, 2016)—which lead to its destruction. Although lithospheric mantle thinning is common and the destruction of the Wyoming Craton in North America has been determined to take place in the Mesoproterozoic (Carlson et al., 2005; Sleep, 2005; Lee et al., 2011), the Mesozoic destruction of the North China Craton is unique and thus has important implications for global continental dynamics (Zhu et al., 2012a).

The spatio-temporal distribution, mechanisms and dynamics of the cratonic destruction in North China have been determined by systematic observations of geology and geophysics as well as studies of experimentation and theoretical modelling (Zhu et al., 2012a). The peak time for the destruction of the North China Craton has been constrained to occur at 130–120 Ma in the early Cretaceous (Zhu et al., 2012b). The destruction basically occurred in the eastern part of the North China Craton and was mainly triggered by subduction of the Paleo-Pacific plate (Zhu et al., 2012a); the western part of the North China Craton was not modified (Zhu et al., 2011). The possible physicochemical mechanisms for the destruction of the eastern North China Craton include thermo-chemical erosion (Menzies et al., 1993; Xu, 2001; Zheng et al., 2001), lithospheric delamination (Gao et al., 2002, 2004, 2008, 2009; Deng et al., 2004; Wu et al., 2005; Xu W L et al., 2013), melt-peridotite interactions (Liu et al., 2005, 2008, 2010; Zhang, 2005, 2009) and hydration (Niu, 2005). These mechanisms may have occurred at different stages or in different regions. A common signature of these mechanisms is related to diverse melt/fluid-peridotite interactions. Therefore, it is of great importance to decipher the mechanism for the destruction of the eastern North China Craton, to recognize the origin, signature and spatio-temporal distribution of the melt/fluid activity in the lithospheric mantle.

Based on the water content of clinopyroxene phenocrysts in the Mesozoic Feixian basalt (125 Ma), Xia et al. (2013) calculated a high water content for the lithospheric mantle source, which may have significantly reduced the viscosity of the lithospheric mantle and provided a prerequisite for the removal of the cratonic root in eastern North China. Numerical modeling suggests that perturbation of the strongly hydrous mantle transition zone, caused by slab flattening and stagnation, could trigger cratonic destruction and removal of the lithospheric root (Wang Z S et al., 2016). Zhang (2009) emphasized that melt-peridotite interactions are crucial to the destruction of cratonic lithospheric mantle. However, an orthopyroxene-rich zone may be formed in the reaction front of silicate melt-peridotite interactions under dry hydrostatic conditions (Rapp et al., 1999; Wang et al., 2010; Zhang J F et al., 2012; Wang C G et al., 2013) and an amphibole-rich zone may be formed under hydrous conditions (Gervasoni et al., 2017). Therefore, the silicate melt-peridotite interactions are sluggish, self-restrained processes, athough these interactions can be promoted by tectonic deformation (Zhang J F et al., 2012).

Compared with silicate melts, carbonate melts have a lower density and lower viscosity, but a higher reactivity, and are considered to be an effective agent for mantle metasomatism (Green and Wallace, 1988; Ionov et al., 1993b; Yaxley et al., 1998; Blundy and Dalton, 2000; Hammouda and Laporte, 2000; Grassi and Schmidt, 2011; Sokol et al., 2016; Gervasoni et al., 2017). The experimental results of Wang C et al. (2016) indicate that carbonate melts derived from a subducted slab can significantly modify and destroy cratonic lithospheric mantle. Slab subduction may also carry carbonate sediments into the deep mantle, with only a limited amount of carbonate being released during decarbonation at shallow depths (Yaxley and Green, 1994; Molina and Poli, 2000; Kerrick and Connolly, 2001; Dasgupta et al., 2005; Liu Y S et al., 2015; Chen C F et al., 2016). Therefore, large amounts of carbonate sediment remnants may be stored in the deep mantle or transformed into carbonate melts by partial melting (Wallace and Green, 1988; Dasgupta et al., 2005). Since the Paleozoic, the southward, northward and westward subductions of the Paleo-Asian plate, the Paleo-Tethyan plate and the Paleo-Pacific plate, respectively, would have resulted in multiple modifications of the North China Craton over long periods of time (Windley et al., 2010). These subducted slabs may also have carried large amounts of carbonate sediments into the deep mantle (Liu Y S et al., 2015; Chen C F et al., 2016; Zhang et al., 2017), inducing extensive carbonate metasomatism of the lithospheric mantle and providing a prerequisite for the destruction of the North China Craton. We provide here a systematic summary of the spatio-temporal variations of carbonate metasomatism in the lithospheric mantle beneath the eastern

North China Craton and try to establish a possible link between carbonate metasomatism and cratonic destruction.

## 2. Occurrence of lithospheric mantle samples in the eastern North China Craton

Numerous mantle peridotite xenoliths have been found in Paleozoic kimberlites and Jurassic-Quaternary volcanic rocks in the eastern North China Craton (Figure 1). Some mantle-derived peridotite terranes also occur in the Triassic Sulu ultrahigh pressure (UHP) belt (Figure 1). These mantle peridotites can be used to constrain the evolution of the lithospheric mantle before and after the destruction of the eastern North China Craton (Zheng, 2009). The Paleozoic mantle peridotite xenoliths hosted in the Mengyin, Fuxian and Tieling kimberlites (Gao et al., 2002; Wu et al., 2006; Zheng et al., 2006, 2007) and the Triassic Sulu orogenic mantle peridotite terranes (Zheng et al., 2005b, 2006; Yuan et al., 2007; Zhang Z M et al., 2011; Su et al., 2016) have undergone strong serpentinization, which makes it difficult to determine their protoliths, although they are all ancient and refractory with Re-depletion Os model ages ($T_{RD}$) of 3.2–1.5 Ga (Figure 2). The Jurassic Xinyang and early Cretaceous Tietonggou mantle peridotite xenoliths consist of refractory harzburgites and dunites (Zheng et al., 2005a; Xu et al., 2008) and represent ancient lithospheric mantle before the destruction of the North China Craton. The 4 Ma Hebi mantle peridotite xenoliths are dominated by harzburgites with $T_{RD}$ ages of 3.0–1.8 Ga and are also considered as representative of the ancient and refractory lithospheric mantle beneath the North China Craton (Zheng et al., 2001, 2007; Sun et al., 2012).

The mantle peridotite xenoliths hosted in the late Cretaceous Fuxin (~100 Ma), Qindao Pishikou (86–78 Ma) and Junan (67 Ma) basalts, the Neogene Shanwang (18 Ma), Changle (19 Ma), Qixia (18–4 Ma) and Penglai (6–4 Ma) basalts and the Quaternary Huinan (<0.6 Ma), Kuandian (<0.6 Ma) and Nushan (<0.7 Ma) basalts, which are formed after the destruction of the eastern North China Craton and


**Figure 1** Distribution of mantle-derived peridotite xenoliths and terranes in the eastern North China Craton.

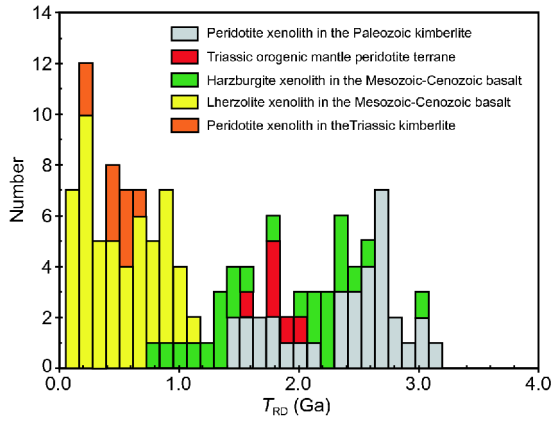


**Figure 2** Cumulative probability plot of Re-depletion Os model ages ($T_{RD}$) of the Paleozoic-Cenozoic lithospheric mantle xenoliths and terranes in the eastern North China Craton. Data are from Gao et al. (2002), Wu et al., (2006), Yuan et al. (2007), Zheng et al. (2007), Chu et al. (2009), Yang et al. (2010), Sun et al. (2012) and Su et al. (2016).

are dominated by fertile lherzolites with a few refractory harzburgites (Figure 1). These lherzolites have much younger $T_{RD}$ ages than the harzburgites (Figure 2). We therefore conclude that the lherzolites in the eastern North China Craton represent new, fertile lithospheric mantle and the harzburgite xenoliths represent ancient, refractory mantle. Mantle peridotite xenoliths hosted in Triassic (223 Ma) kimberlites and Neogene (6.6 Ma) basalts from North Korea have previously been suggested to represent new and fertile lithospheric mantle, athough no petrological classification was available (Yang et al., 2010).

## 3. Geochemical indices of cryptic carbonate metasomatism in the lithospheric mantle

Mantle-derived peridotite xenoliths in volcanic rocks and terranes in orogenic belts provide direct samples of the lithospheric mantle, giving an important window with which to observe mantle metasomatism (Bodinier et al., 2003; Pearson et al., 2003). Most mantle metasomatism is cryptic metasomatism describing changes in composition of pre-existing minerals without the formation of new phase. Therefore, some special geochemical indices in minerals are useful to decipher cryptic mantle metasomatism of the lithospheric mantle. By combining elemental partitioning coefficients between carbonate melts and silicate minerals with the elemental signatures of carbonatites, Rudnick et al. (1993) suggested that high La/Yb, Nb/La, Ca/Al and Zr/Hf ratios and low Ti/Eu ratios are effective geochemical indices for tracing carbonate metasomatism in the mantle. Klemme et al. (1995) reported that Ti/Eu is more sensitive to carbonate metasomatism. Coltorti et al. (1999) used $(La/Yb)_N$ and Ti/Eu ratios in clinopyroxene to distinguish carbonate metasomatism from silicate metasomatism (Figure 3a). On the basis of published geochemical data at that time, Coltorti et

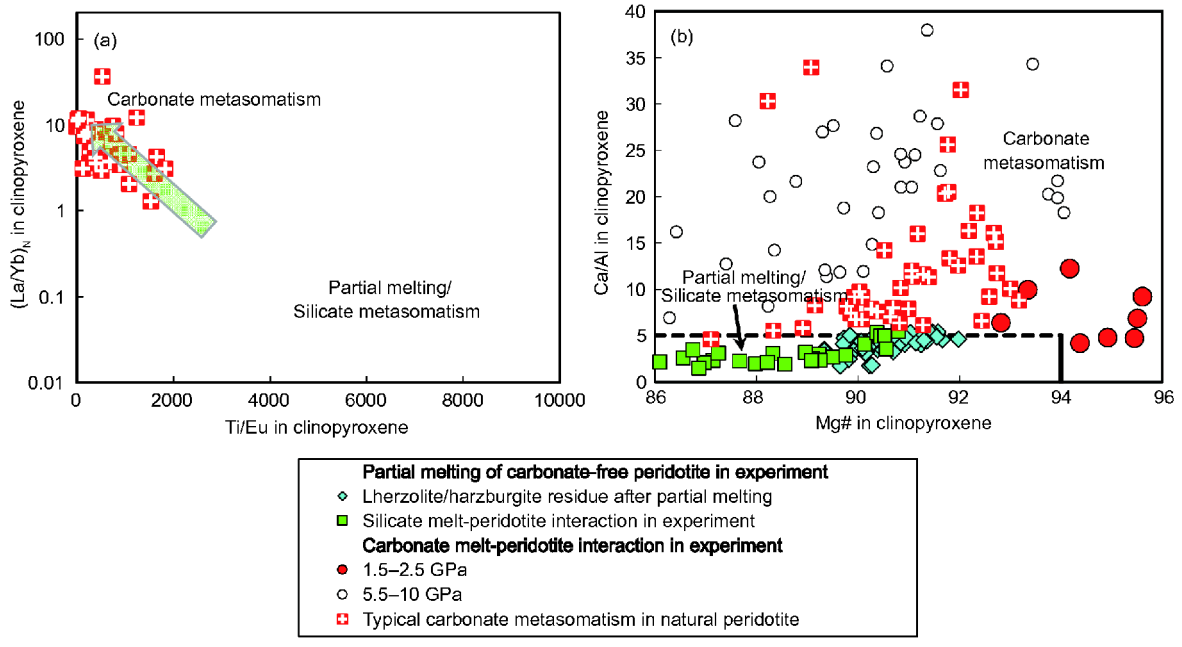


**Figure 3** Variations of (a) $(La/Yb)_N$ with Ti/Eu (modified from Coltorti et al. (1999)) and (b) Ca/Al with Mg# in clinopyroxene from natural and experimental mantle peridotite. Experimental data for the partial melting of carbonate-free peridotite are from Walter (1998), Gaetani and Grove (1998), Pickering-Witter and Johnston (2000), Falloon et al. (1999), Baker and Stolper (1994), Wasylenki et al. (2003) and Schwab and Johnston (2001) (only experiments with lherzolite and harzburgite residue were selected), the data for high-silicate melt-peridotite interactions are from Wang et al. (2010) and Yaxley and Green (1998) and the data for carbonate melt-peridotite interactions are from Dalton and Wood (1993), Brey et al. (2008), Klemme et al. (1995), Sokol et al. (2016) and Gervasoni et al. (2017). The data for typical carbonate metasomatism in nature are from Coltorti et al. (1999), Yaxley et al. (1998) and Neumann et al. (2002).

al. (1999) suggested that the clinopyroxene that results from carbonate metasomatism is generally characterized by $(La/Yb)_N$>3–4 and Ti/Eu<1500, although these are not absolute values. Figure 3 shows that some clinopyroxenes resulting from typical carbonate metasomatism have Ti/Eu rstios close to 2000 and $(La/Yb)_N$ values<3. We therefore suggest that the trends of $(La/Yb)_N$ and Ti/Eu in clinopyroxene may be used to distinguish carbonate metasomatism from silicate metasomatism (Figure 3a). However, despite the rapid development of *in situ* analyses that could be used to apply this trace element index to trace carbonate metasomatism in the lithospheric mantle (Zheng et al., 2007; Sun et al., 2012; Deng et al, 2017), there is only a limited amount of published data on the trace elemental contents of minerals from the North China Craton. This has hindered the systematic spatio-temporal assessment of carbonate metasomatism in the lithospheric mantle in this region.

Carbonate melts have very high Ca/Al ratios (Rudnick et al., 1993) and both Ca and Al are stoichiometric elements of clinopyroxene. Thus, the Ca/Al ratio of clinopyroxene can be considered as an effective major elemental index to trace carbonate metasomatism in the lithospheric mantle. Figure 3b shows the variation of the major element (Ca/Al and Mg#) composition of clinopyroxene in natural and experimental mantle peridotites. Clinopyroxene in lherzolite and harzburgite after partial melting (Baker and Stolper, 1994; Gaetani and Grove, 1998; Walter, 1998; Falloon et al., 1999; Pickering-Witter and Johnston, 2000; Schwab and Johnston, 2001; Wasylenki et al., 2003) and the interactions between experimental eclogite-derived high-silicate melts and peridotites (Wang et al., 2010; Yaxley and Green, 1998) show the low Ca/Al ratios <5 and Mg# values <92 (Figure 3b). However, most of the Ca/Al ratios are >5 in clinopyroxene formed during experimental carbonate melt-peridotite interactions (Figure 3b) (Dalton and Wood, 1993; Klemme et al., 1995; Brey et al., 2008; Sokol et al., 2016; Gervasoni et al., 2017). All the clinopyroxenes resulting from natural carbonate metasomatism show high Ca/Al ratios >5 (Figure 3b). We therefore conclude that a Ca/Al ratio >5 is an important geochemical index with which to trace carbonate metasomatism in the lithospheric mantle. Major element contents, including Ca and Al, are commonly reported in mantle clinopyroxenes from the North China Craton. Clinopyroxene is also the main carrier of trace elements and has very high Sr and very low Rb contents, making it an ideal mineral for *in situ* Sr isotope analysis (Malarkey et al., 2011; Tong et al., 2016). The very low Rb/Sr ratio means the neglected radiogenic Sr in clinopyroxene that can be used to record the initial Sr isotopic composition in order to constrain the metasomatic agent. We therefore used a comprehensive combination of major element (Ca/Al and Mg#), trace element (Ti/Eu and $(La/Yb)_N$) indices and Sr isotopic compositions of clinopyroxene (Figures 4–6) to study the spatio-temporal variations of carbonate metasomatism in the lithospheric mantle beneath the eastern North China Craton.

## 4. Widespread carbonate metasomatism in the lithospheric mantle beneath the North China Craton

The existence of carbonate melt in the deep mantle is a prerequisite for carbonate metasomatism in the lithospheric mantle. Carbonate melt may be erupted at the surface as carbonatite or may be completely exhausted during interactions with peridotite. Proterozoic and Mesozoic carbonatites are exposed at more than ten locations in the North China Craton. The Meso-Proterozoic Bayan Obo (1.3 Ga), Fengzhen (1.8–1.7 Ga), Huaian (1.8 Ga) and Fangcheng (0.79 Ga) carbonatites have depleted Sr-Nd isotopic compositions ($^{87}Sr/^{86}Sr_{(t)}$=0.7028–0.7031; $\varepsilon_{Nd(t)}$=−1.2 to −6.1). However, the Mesozoic Zhuolu (239 Ma), Songxian (209 Ma), Huairen (229 Ma), Linxian (132 Ma), Huayin (205 Ma), Luonan (221 Ma) and Laiwu (124 Ma) carbonatites show evolved Sr-Nd compositions ($^{87}Sr/^{86}Sr_{(t)}$=0.7043–0.7106; $\varepsilon_{Nd(t)}$=−2.1 to −18.2) (Yan et al., 2007), indicating that these carbonatites were derived from enriched mantle sources or recycled crust. Kim et al. (2016) suggested that the evolved Sr-Nd isotopic compositions ($^{87}Sr/^{86}Sr_{(t)}$=0.703–0.706; $\varepsilon_{Nd(t)}$=−26) of the Mesozoic Hongcheon carbonatite (~230 Ma) in the South Korea is a result of an ancient enrichment event in the lithospheric mantle.

Ying et al. (2004) proposed that the enriched signature of the Mesozoic (124 Ma) Laiwu-Zibo carbonatites is related to the subduction, with continental material, of the South China Block into the deep mantle beneath the North China Craton. Chen C F et al. (2016) reported that the carbonatite intrusion in the late Tertiary Hannuoba basalt has the geochemical characteristics of carbonate sediments, which could be the result of subduction of the Paleo-Asian oceanic plate. Zhang et al. (2017) found the same carbonate melt from the Miocene basalts in the Dongbahao region (Inner Mongolia) along the northern margin of the North China Craton, where two-stage carbonate metasomatism related to the subduction of the Paleo-Asian oceanic plate was proposed for xenoliths of mantle peridotites (Chen et al., 2017; Wu et al., 2017). The Dalihu carbonatite in the Central Asian Orogenic Belt (CAOB) has a similar trace element and oxygen isotopic ($\delta^{18}O_{SMOW}$=20.7–21.5) composition to sedimentary carbonates and contains microscopic diamonds; this is the first direct evidence of sedimentary carbonate recycling during subduction of the Paleo-Asian oceanic plate (Liu Y S et al., 2015). Thus, the presence of widespread subduction-related carbonate melts suggests the possibility of intense carbonate metasomatism in the lithospheric mantle beneath the North China Craton.

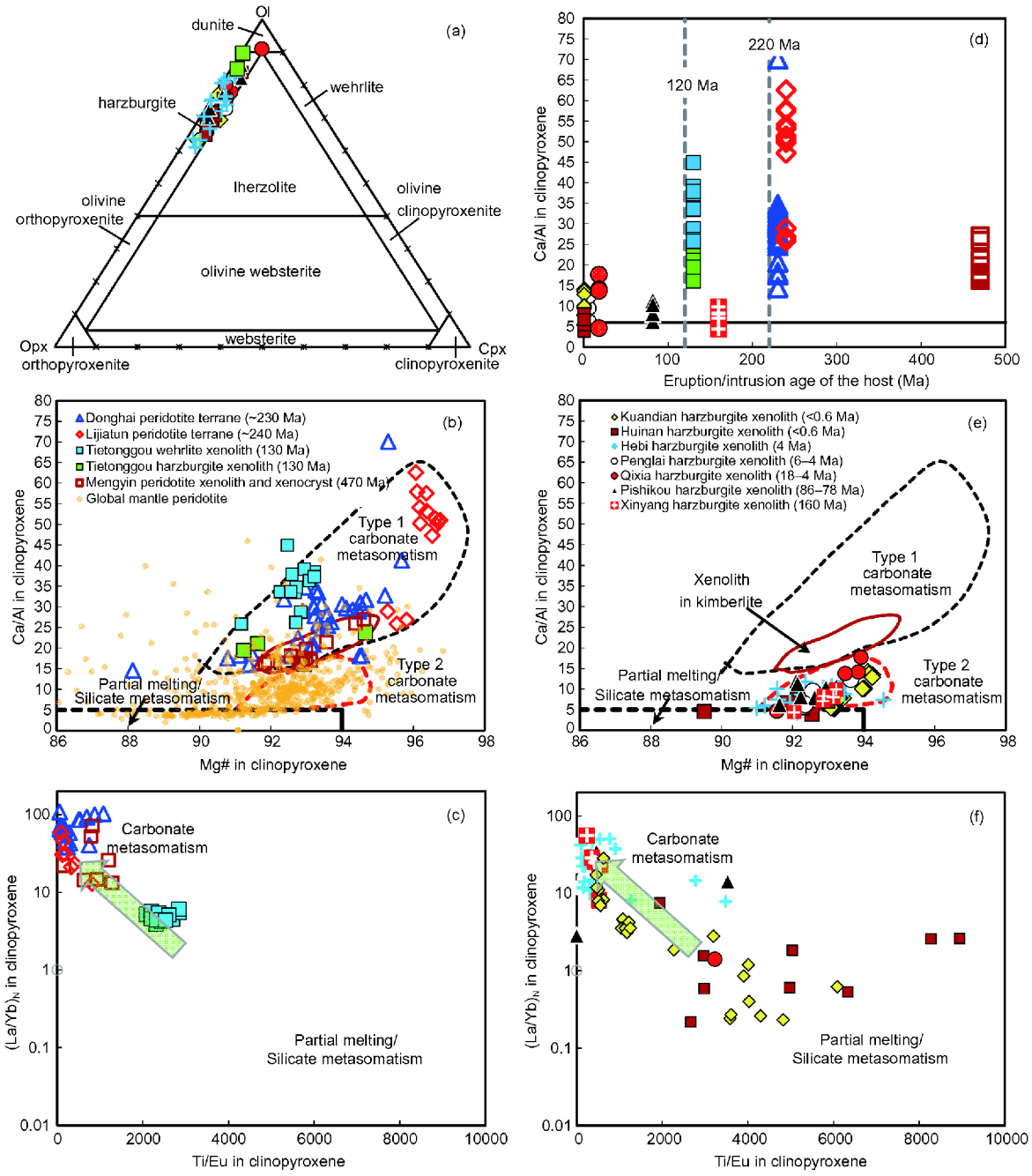


**Figure 4** (a) Petrological classification of harzburgite xenoliths and terranes, variations of the ((b), (e)) Ca/Al ratio with Mg# and ((c), (f)) the $(La/Yb)_N$ with the Ti/Eu in clinopyroxene, and (d) variation of the Ca/Al of clinopyroxene with time in the eastern North China Craton. Except for the strongly serpentinized Mengyin and Xinyang peridotite xenoliths and the Sulu orogenic peridotite terrane, detailed mineral counting work has been carried out on the other harzburgites. The Kuandian data are from Xu et al. (2013b); the Huinan data are from Xu et al. (2003b); the Hebi data are from Zheng et al. (2001); the Penglai data are from Chu et al. (2009); the Qixia data are from Zheng et al. (1998); the Pishikou data of the Qingdao are from Zhang (2009); the Xinyang data are from Zheng et al. (2005a); the Tietonggou data are from Xu et al. (2008) and Zhou et al. (2013); the Lijiatun date are from Su et al. (2016); the Zhimafang, Xugou and Jiangzhuang data in the Donghai are from Yang and Jahn (2000), Zheng et al. (2005b, 2006), Yuan et al. (2007) and Zhang Z M et al. (2011). Data for the South Africa Craton are from Boyd et al. (2004), Franz et al. (1996), Gregoire (2003, 2005), Saltzer (2001), Simon et al. (2003), Stiefenhofer et al. (1997) and Whitehead et al. (2002); data for the Greenland Craton are from Bernstein et al. (1998), Bizzarro and Stevenson (2003), Hellebrand and Snow (2003) and Holm and Prægel(2006); data for the Slave Craton are from Aulbach et al. (2004), Kopylova and Caro (2004), McCammon and Kopylova (2004), Menzies et al. (2004), van Achterbergh et al. (2004), Kopylova et al. (1999), MacKenzie and Canil (1999), Schmidberger and Francis (1999), Shi et al. (1998), Schmidberger et al. (2003), Schmidberger and Francis (2001), Peslier (2002) and Griffin et al. (1999); data for the Siberian Craton are from Ionov et al. (1993a, 2005a, 2005b, 2005c, 2006), Ionov and Hofmann (1995), Griffin et al. (1996), Boyd et al. (1997), Litasov et al. (2000), Ionov (2004), Griffin et al. (2005) and Sharygin et al. (2007); data for the Australia Craton are from Ghorbani and Middlemost (2000), Bruce et al. (2000), Powell et al. (2004), Roach (2004), Woodland et al. (2004), Yaxley et al. (1997, 1998), Eggins et al. (1998), Varela et al. (1999) and Yaxley and Kamenetsky(1999); data for the Wyoming Craton are from Downes (2004) and Carter Hearn (2004); data for the Tanzania Craton are from Dawson (2002) and Lee et al. (2000).

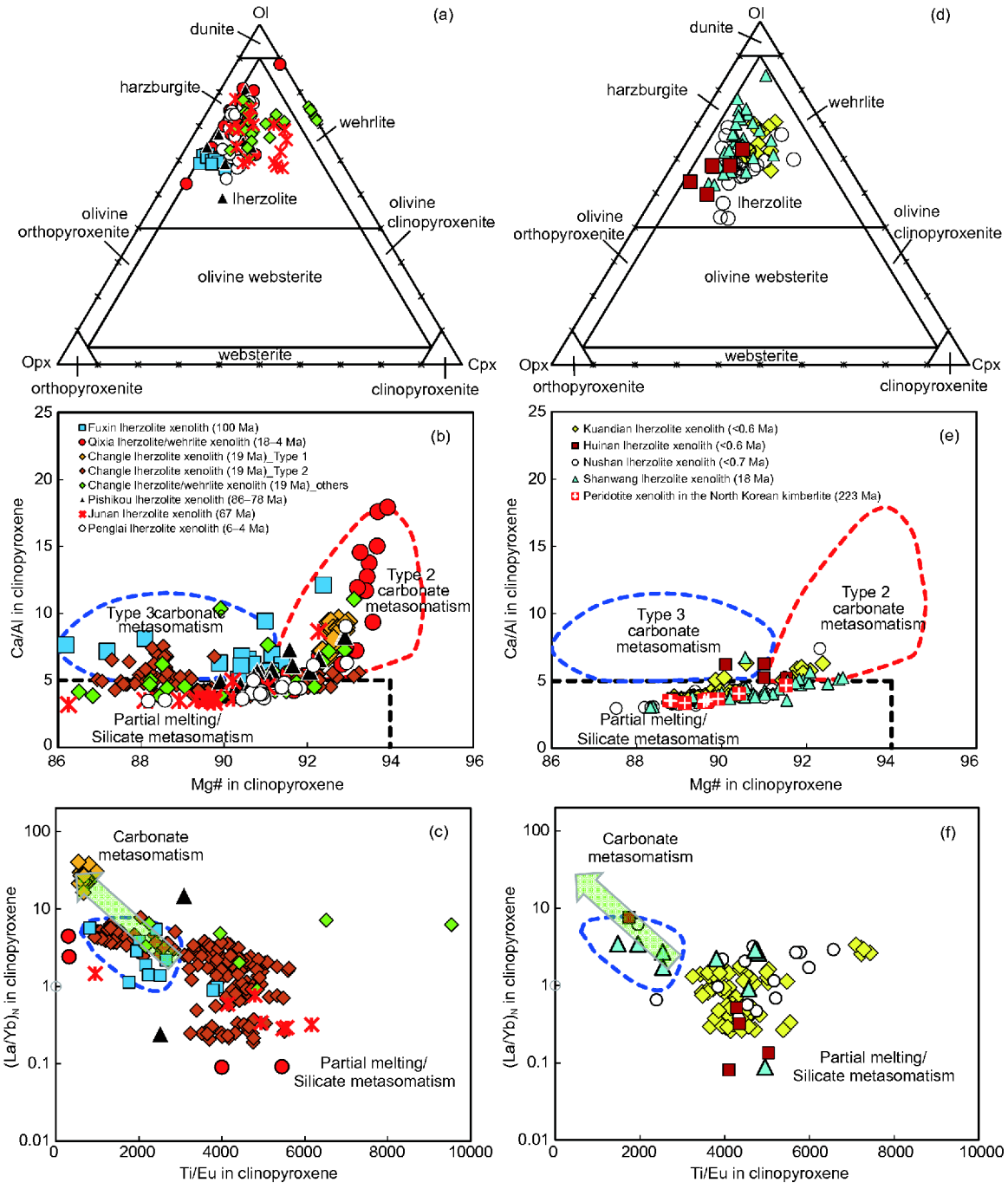


**Figure 5** ((a), (d)) Petrological classification of the late Cretaceous to Quaternary lherzolite/wehrlite xenoliths. ((b), (e)) Variations of the Ca/Al ratio with Mg# and ((c), (f)) the $(La/Yb)_N$ ratio with the Ti/Eu in clinopyroxene of the eastern North China Craton. The Fuxin data are from Zheng et al. (2007); the Qixia data are from Zheng et al. (1998) and Xia et al. (2010); the Changle data are from Xiao et al. (2010) and Deng et al. (2017); the Pishikou data of the Qingdao are from Zhang (2009); the Junan data are from Ying et al. (2006) and Zhang (2009); the Penglai data are from Chu et al. (2009) and Xia et al. (2010); the Kuandian data are from Xu R et al. (2013a, 2013b); the Huinan data are from Xu et al. (2003a, 2003b); the Nushan data are from Xu et al. (1998) and Xu et al. (2000); the Shanwang data are from Zheng et al. (1998, 2006) and Chu et al. (2009); Data for the peridotite xenoliths in the North Korea are from Yang et al. (2010).

The elemental and isotopic compositions of mantle-derived mafic and ultramafic rocks can be used to indirectly constrain their mantle sources (Hofmann, 1997). Mesozoic to Cenozoic basalts are widely distributed in the North China Craton (Liu et al., 2008; Zheng et al., 2018). Based on a detailed elemental study, Zeng et al. (2010) proposed that the mantle source of the Cenozoic alkaline basalts in the Shandong Province was dominated by carbonated peridotite. Melt inclusions in the olivine phenocrysts of alkaline basalts from Yangzhuang in the Shandong Province contain methane

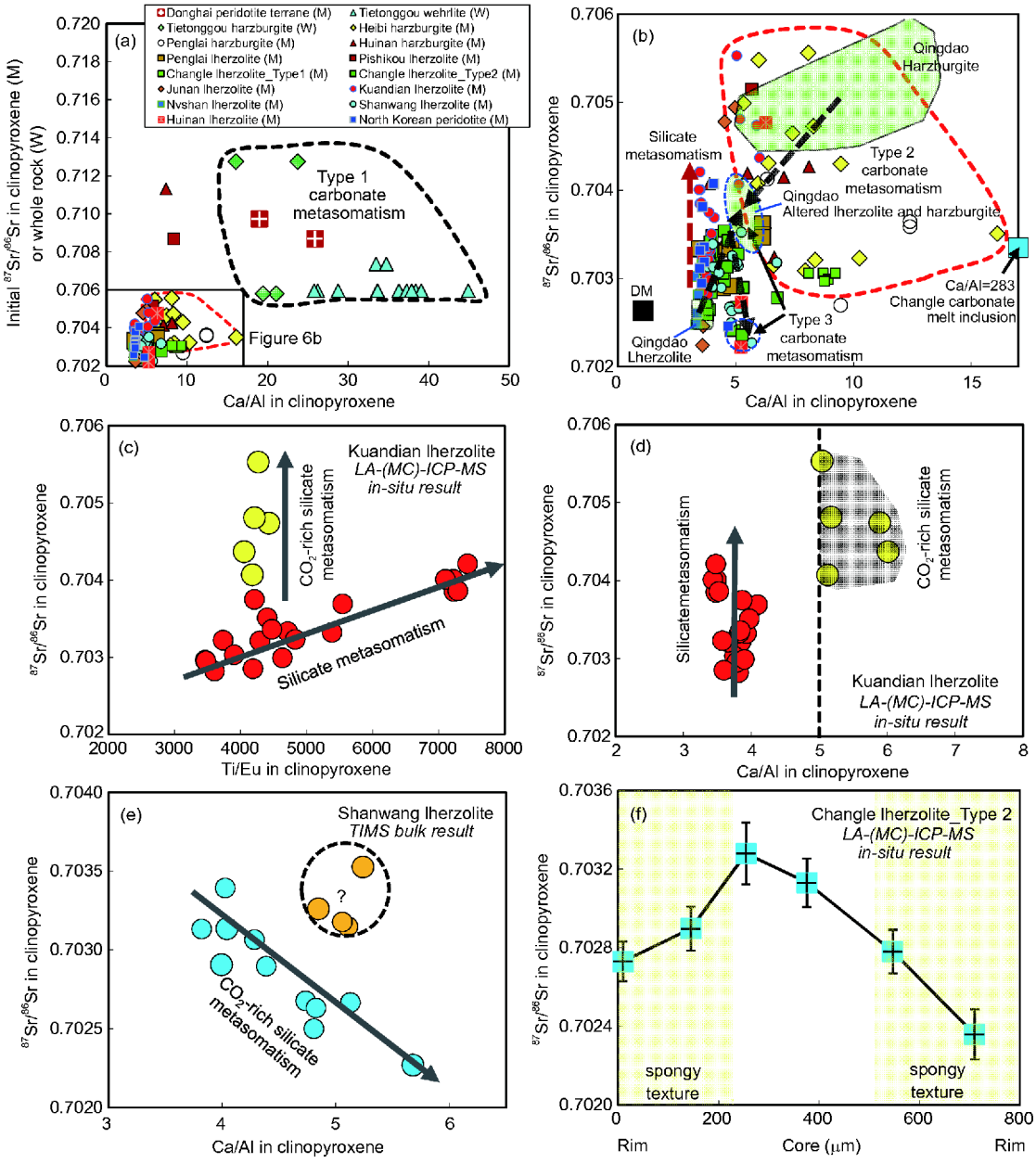


**Figure 6** ((a), (b)) Variations of the Ca/Al ratio with Sr isotopic composition in clinopyroxene of the peridotite xenoliths from the eastern North China Craton. ((c), (d)) Variations of Sr isotopic composition with the Ti/Eu and Ca/Al ratios of clinopyroxene in the Kuandian lherzolite xenolith. (e) Variations of Sr isotopic composition with the Ca/Al ratio in clinopyroxene of the Shanwang lherzolite xenolith. (f) Sr isotopic profile of clinopyroxene in the Changle Type 2 lherzolite xenolith. Data for the Donghai orogenic peridotite terrane are from Yang and Jahn (2000); the Tietonggou data are from Xu et al. (2008) and Zhou et al. (2013); Hebi data are from Sun et al. (2012); the Penglai data are from Chu et al. (2009); the Huinan data are from Xu et al. (2003b); the Pishikou data of the Qingdao are from Zhang et al. (2009); the Changle data are from Xiao et al. (2010) and Deng et al. (2017); the Junan data are from Zhang (2009); the Kuandian data are from Xu et al. (2013a); the Nushan data are from Xu et al. (2000); the Shanwang data are from Chu et al. (2009); Data for the North Korea are from Yang et al. (2010).

($CH_4$) and other hydrocarbons and some carbonaceous minerals such as graphite and carbonate, indicating a carbonated mantle source (Liu F et al., 2015). Late Cretaceous to Cenozoic basalts in eastern China are characterized by light Mg isotope and heavy Zn isotope compositions, which has been suggested to be a result of the westward subduction of the Pacific oceanic plate and the recycling of carbonate sediments into the mantle (Yang W et al., 2012; Liu et al., 2016; Li et al., 2017).

Triassic low-Si alkaline rocks occur widely along the northern margin of the North China Craton and are considered to represent a low degree of partial melting of metasomatosed and enriched mantle (Yan et al., 2001; Niu et al., 2012; Yang J H et al., 2012; Zhang S H et al., 2012). These alkaline rocks show a crustal elemental and Sr-Nd isotopic signature that is different in comparism to the asthenospheric

mantle. Thus, the metasomatic melt/fluid is contributed to recycling of the crust (Yan et al., 2002; Zhu et al., 2017). The presence of carbonate veins and intergranular calcite in the Fanshan alkaline complex suggest that the original magma contained certain amounts of $CO_2$ (Yan et al., 2007; Niu et al., 2012). The very high Ca content in the early crystallized clinopyroxene is consistent with Ca enrichment in the original magma, which could be derived from a carbonated mantle source (Niu et al., 2012; Hou et al., 2015) resulting from subduction of the Paleo-Asian oceanic plate (Niu et al., 2017).

Carbonate minerals such as calcite, dolomite and magnesite can be formed during carbonate metasomatism (Yaxley et al., 1991; Ionov et al., 1993b, 1996; Rudnick et al., 1993). These index minerals can therefore be used directly to identify carbonate metasomatism. Intergranular calcite grains have been found in peridotite xenoliths from the Changle basalts in the eastern North China Craton (Xiao et al., 2010; Deng et al., 2017) and the Datong basalts in the Trans-North China Orogen (TNCO) (Wang C Y et al., 2016). Carbonate melt inclusions hosted in olivine and clinopyroxene were also present in the Changle peridotite xenolith (Deng et al., 2017). Carbonate metasomatism is always accompanied by the formation of secondary clinopyroxene (Ionov et al., 1993b; Coltorti et al., 1999; Sun et al., 2012), which is formed during the reaction of carbonate melts with orthopyroxene (Dalton and Wood, 1993). Wehrlites composed of olivine and clinopyroxene are therefore considered to be the end-product of carbonate metasomatism in the lithospheric mantle (Yaxley et al., 1991, 1998; Rudnick et al., 1993; Neumann et al., 2002). Wehrlite samples have been reported in Cenozoic Changle peridotite xenoliths (Xiao et al., 2010) and early Cretaceous high-Mg diorites from the western Shandong Province (Zhou et al., 2013) in the eastern North China Craton.

Orogenic mantle peridotite terranes in the Triassic Sulu orogenic belt are generally considered to be fragments of the lithospheric mantle of the North China Craton that have been carried to crustal depths during the exhumation of the deeply subducted South China Block (Zheng et al., 2006; Zhang R Y et al., 2008, Zheng Z M et al., 2011; Su et al., 2016). Magnesite and dolomite are common accessory minerals in the Donghai garnet-bearing mantle peridotite in the southern Sulu orogenic belt, in which ~225 Ma metamorphic zircon grains contain magnesite and $CO_2$ fluid inclusions (Zheng Z M et al., 2011). In the northern Sulu orogenic belt, the Lijiatun spinel-bearing mantle peridotite includes intergranular dolomite, in which (clinopyroxene+olivine) veins with wehrlite mineral assemblage crosscutting orthopyroxene porphyroblasts are considered as the direct evidence of carbonate metasomatism (Su et al., 2016). Based on the geochemical indices $(La/Yb)_N$ and Ti/Eu of clinopyroxene, Zheng et al. (2007) suggested that the lithospheric mantle beneath the North China Craton experienced carbonate metasomatism in the Paleozoic and early Mesozoic, but silicate metasomatism in the late Mesozoic and Cenozoic. In this study, however, we showed that three different types of carbonate metasomatism with spatio-termporal variations can be identified in the Paleozoic to Cenozoic lithospheric mantle beneath the eastern North China Craton on the basis of major element (Ca/Al and Mg#) and trace element (Ti/Eu and $(La/Yb)_N$) indices and the Sr isotope composition of mantle clinopyroxene (Figures 4–6).

## 5. Temporal variations of carbonate metasomatism in the lithospheric mantle beneath the eastern North China Craton

Carbonate metasomatism characterized by the high Ca/Al, Mg# and $(La/Yb)_N$ and low Ti/Eu ratios of clinopyroxene is recorded by harzburgite xenoliths in the volcanic rocks, orogenic mantle peridotites in the Triassic Sulu UHP belt and mantle peridotite xenoliths and xenocrysts in the Paleozoic kimberlites of the eastern North China Craton, although not in the Huinan harzburgite xenoliths (Figure 4). The high Ti/Eu ratios in the clinopyroxenes of the Huinan harzburgite (Figure 4f) are results of the interactions of basaltic melts and peridotites (Xu et al., 2003a, 2003b). However, the slightly high Ca/Al ratio of 4–8 in clinopyroxene is consistent with a carbonate overprint or a small amount of metasomatims by a volatile-rich melt (Xu et al., 2003a). This further indicates that a comprehensive consideration of the major (e.g., Ca/Al) and trace (e.g., Ti/Eu) element geochemical indices in clinopyroxene is effective in tracing carbonate metasomatism in the lithospheric mantle.

Clinopyroxene in the Triassic Sulu orogenic peridotites has a very high Ca/Al ratio (median 29), which is defined as Type 1 carbonate metasomatism, whereas the median Ca/Al ratios of clinopyroxene in the Paleozoic Mengyin peridotite xenoliths and the global cratonic lithospheric mantle are 17 and 10, respectively (Figure 4b). Apart from the early Cretaceous Tietonggou harzburgites and wehrlites with records of Type 1 carbonate metasomatism, the Ca/Al ratio in the clinopyroxene of harzburgite xenoliths hosted in the Jurassic to Cenozoic volcanic rocks decreases to 5–18, indicative of Type 2 carbonate metasomatism (Figure 4e). However, based on the geochemical signature of natural carbonatites (Rudnick et al., 1993) and the elemental partitioning of experimental carbonate melts (Klemme et al., 1995), mantle-derived magma can inherit the geochemical indices of a carbonated mantle source, such as high Ca/Al and $(La/Yb)_N$ and low Ti/Eu ratios (Zeng et al., 2010). The Ca/Al and $(La/Yb)_N$ ratios are higher and the Ti/Eu ratio is lower in the Triassic mafic rocks of the Jiaodong Peninsula than those of the Cretaceous and Cenozoic mafic rocks of the eastern

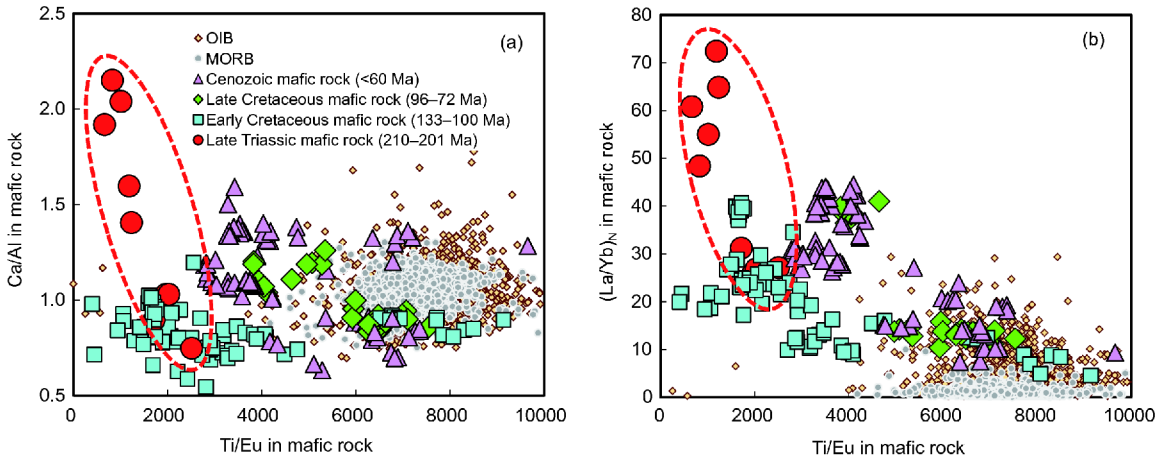


**Figure 7** (a) Variations of the Ca/Al ratio with the Ti/Eu ratio and (b) the $(La/Yb)_N$ with the Ti/Eu ratio in Mesozoic-Cenozoic mafic rocks from the eastern North China Craton. Data for the eastern North China Craton are from Dai et al. (2016), Liu et al. (2008) and Zeng et al. (2010). The mid-ocean ridge basalt (MORB) data are from Gale et al. (2013); the oceanic island basalt (OIB) data are from http://georoc.mpch-mainz.gwdg.de/georoc/. Only MgO >7.5% data are used in this study.

North China Craton (Figure 7). Therefore, we conclude that carbonate metasomatism in the eastern North China Craton was transformed from Type 1 to Type 2 during the Triassic period (Figure 4d), which is consistent with Type 1 and Type 2 carbonate metasomatisms showing the striking $^{87}Sr/^{86}Sr$ composition of clinopyroxene of 0.706–0.713 and 0.703–0.706, respectively (Figure 6a).

After the peak decratonization of the eastern North China Craton, the clinopyroxene of the 100 Ma Fuxin peridotite xenolith and some Tertiary Changle lherzolite xenoliths were characterized by the relatively high Ca/Al ratios (>5), but low Mg# signatures. This is defined as Type 3 carbonate metasomatism (Figure 5b). Type 3 carbonate metasomatism also displays by medium Ti/Eu ratios (~1000–3000) and slightly high $(La/Yb)_N$ ratios in clinopyroxene and plots in the transitional domain between typical carbonate metasomatism and silicate metasomatism (Figure 5c).

## 6. Spatial variations of carbonate metasomatism in the lithospheric mantle beneath the eastern North China Craton

Partial melting of the upwelling asthenosphere generally produces silicate-rich melts that induce silicate metasomatism and form juvenile lithospheric mantle during thinning of the lithospheric mantle (Xu et al., 2003b). However, the juvenile lithospheric mantle in the eastern North China Craton is overprinted by carbonate metasomatism with obvious spatial variations. Lherzolite xenoliths with Type 2 and Type 3 carbonate metasomatism are mainly found in the Jiaodong Peninsula, whereas silicate metasomatism is seen far from the Jiaodong Peninsula in the eastern North China Craton. Clinopyroxenes in some lherzolite xenoliths from the Qixia, Penglai, Qingdao, Changle (Type 1 lherzolite) and Junan in the Jiaodong Peninsula and surrounding areas show element signatures of Type 2 carbonate metasomatism (high Ca/Al ratios and Mg#; low Ti/Eu ratios) (Figure 5b and c). These lherzolites show the same Sr isotopic composition as the harzburgites that experienced Type 2 carbonate metasomatism, with $^{87}Sr/^{86}Sr$ ratios of 0.703–0.705 and 0.703–0.706, respectively (Figure 6b). Type 3 carbonate metasomatism has only been recorded by a few lherzolite xenoliths (Figure 5e and f) and the $^{87}Sr/^{86}Sr$ ratio shows a negative relationship with the Ca/Al in clinopyroxene for most lherzolite xenoliths (Figure 6e) from the Shanwang, indicating that the carbonate metasomatic agent may have been derived from very depleted asthenospheric mantle ($^{87}Sr/^{86}Sr<0.7023$). Such Type 3 carbonate metasomatism with a very low $^{87}Sr/^{86}Sr$ ratio has also been reported in the lherzolite xenoliths from the nearby Changle (Deng et al., 2017) (Figures 5b, 6b and f). However, our unpublished data show that the Qingdao harzburgite and lherzolite xenoliths altered by Type 3 carbonate metasomatism have a relatively high $^{87}Sr/^{86}Sr$ ratio of 0.7033–0.7040 in clinopyroxene with a Ca/Al ratio of 4.1–6.0 (Figure 6b). The Cenozoic lherzolite xenoliths from the Kuandian and Nushan far away from the Jiaodong Peninsula, mainly experienced silicate metasomatism, with very weak or absent carbonate metasomatism (Figure 5e and f). Most of the lherzolite xenoliths from the Kuandian show a clear positive relationship between the $^{87}Sr/^{86}Sr$ ratios (0.7028–0.7042) and Ti/Eu ratios in clinopyroxene (Figure 6c), which is consistent with silicate metasomatism (Xu R et al., 2013a). However, a few lherzolite xenoliths have slightly higher $^{87}Sr/^{86}Sr$ (0.7041–0.7055) and Ca/Al ratios (Figure 6d), very high Ti/Eu ratios (>4000) and no relationship between the Ti/Eu with $^{87}Sr/^{86}Sr$ ratios in clinopyroxene (Figure 6c), indicating a low degree of metasomatism by a $CO_2$-rich silicate melt (Figure 6d).

Therefore, the juvenile lithospheric mantle underneath the Jiaodong Peninsula and surrounding areas has affected by intense carbonate metasomatism, which is spatially consistent with the remarkable lithosphere thinning, large volume of asthenosphere upwelling and giant gold deposits in this region.

## 7. Link of carbonate metasomatism to the destruction of the eastern North China Craton and associated giant gold deposits

A short-lived giant igneous events (135–110 Ma) (Wu et al., 2005; Zhu et al., 2012b; Zhang et al., 2014), tectonic extension(Lin et al., 2013; Zhu et al., 2015) and the formation of giant gold deposits (Yang et al., 2003; Li et al., 2012; Zhu et al., 2015; Fan et al., 2016) are well developed in the early Cretaceous of the eastern North China Craton. Based on two types of mafic igneous rocks from the Jiaodong Peninsula with contrasting geochemical compositions, Dai et al. (2016) suggested that the nature of the mantle lithosphere in the eastern North China Craton changed from an ancient lithospheric mantle to a juvenile lithospheric mantle at ~121 Ma —that is the time of termination of the peak decratonization. As a result of the good spatio-temporal consistence between the destruction of the eastern North China Craton and the westward subduction of the Pacific plate, Paleo-Pacific subduction has been suggested as the main dynamic factor triggering the destruction of the eastern North China Craton and the formation of giant gold deposits (Sun et al., 2007; Zhu et al., 2011, 2012a, 2015).

The westward subduction of the Paleo-Pacific plate not only modified the North China Craton, but also had a significant impact on the architecture of the whole of eastern Asia (Sun et al., 2007; Yin, 2010; Dong et al., 2015). For example, the subduction of the Paleo-Pacific plate induced widespread Cretaceous magmatism (Wang Y J et al., 2013) and extensional tectonism (Lin et al., 2013) in the South China Block, which is a stable craton and lacks Jiaodong/decratonic gold deposits (Deng and Wang, 2016). This suggests that the lithospheric mantle beneath the eastern North China Craton may have had unique characteristics before its destruction in the early Cretaceous. Carboniferous-early Permian (324–270 Ma) and late Permian-Triassic (262–236 Ma) alkaline rocks occur widely on the northern margin of the North China Craton as a result of the subduction of the Paleo-Asian oceanic plate during the late Paleozoic (Zhu et al., 2012b). The southeastern North China Craton was modified by the deep subduction of the South China Block and the formation of the late Triassic (225–210 Ma) post-collision magmatism (Zhu et al., 2012b). The late Triassic peridotite xenoliths hosted by the ~223 Ma North Korea kimberlites are characterized by juvenile lithospheric mantle, which demonstrates that the eastern North China Craton was partially destroyed in the Triassic (Yang et al., 2010).

Long-lived and multiple subduction-related modifications around the North China Craton significantly changed the physical and chemical properties of the lithosphere mantle (Windley et al., 2010), providing a prerequisite for the final decratonization. The westward subduction of the Paleo-Pacific plate in the late Mesozoic simply provided a final driving force for the destruction of the eastern North China Craton. The subducted slab not only contributed the dehydrated water to reduce the strength of the upper lithospheric mantle (Niu, 2005; Windley et al., 2010; Xia et al., 2013), but also triggered subduction-related crustal recycling and melt-peridotite interactions in the lithospheric mantle (Liu et al., 2005, 2010). The low viscosity and low density carbonate melt reacted easily with mantle peridotite and consumed orthopyroxene (Russell et al., 2012; Kamenetsky and Yaxley, 2015), which modified the structure and composition of the lithospheric mantle. Experimental work by Wang C et al. (2016) showed that carbonate melt can very quickly percolate along grain boundaries in harzburgite to form a porridge-like texture, dispersing the cratonic lithospheric mantle.

Compared with the clinopyroxene of global cratonic peridotites, the clinopyroxene in the lithospheric mantle beneath the Sulu orogenic belt and surrounding areas in the eastern North China Craton is characterized by very high Ca/Al ratios (up to 70) before the late Triassic (Figure 4b), which indicates strong Type 1 carbonate metasomatism. The lithospheric mantle therefore had a global unique characteristic before the destruction of the eastern North China Craton. The presence of the clinopyroxene (Ca/Al=47–63) and olivine veins with wehrlite mineral assemblages cross-cutting the orthopyroxene porphyroblasts in the ~240 Ma Lijiatun orogenic peridotite is the direct petrological evidence for strong Type 1 carbonate metasomatism in the lithospheric mantle beneath the eastern North China Craton in the Triassic (Su et al., 2016). In general, carbonate melt can exist in the deep mantle, such as the asthenospheric mantle beneath thick subcontinental lithospheric mantle. However, Type 1 carbonate metasomatism is present in both the Donghai garnet-bearing and the Lijiatun spinel-bearing orogenic peridotites, which implies that the deep and shallow lithospheric mantle beneath the eastern North China Craton was strongly modified by Type 1 carbonate metasomatism before the late Triassic. Such Type 1 carbonate metasomatism can also been identified in the ~130Ma Tietonggou peridotite xenolith before the peak (~125 Ma) decratonization of the eastern North China Craton (Figure 4b and d). However, Type 1 carbonate metasomatism can not be identified in all the peridotite xenoliths that were trapped after the destruction of the eastern North China Craton (Figures 4d, e and 5b, e). Therefore, we suggest that Type 1 carbonate

metasomatism is a prerequisite for the final destruction the eastern North China Craton under global mantle heating in the Cretaceous (Machetel and Humler, 2003) and the mantle convection and destabilization induced by the subduction of the Paleo-Pacific plate (Zhu et al., 2011).

The Jiaodong Peninsula is one of the most important gold deposit provinces in China. It covers <1% of the land area, but accounts for >25% of the total proven gold reserves in China. The Jiaodong gold deposit province was formed within a few million years in the early Cretaceous (130–120 Ma) and was coevally with the peak destruction of the eastern North China Craton and spatially consistent with a pervasive carbonate metasomatism in the lithospheric mantle (Figure 1). Its ore-forming fluids were thought to have been largely derived from a cooling magma and/or from mantle degassing, which is distinct from typical orogenic gold deposits worldwide (Yang et al., 2003; Li et al., 2012; Zhu et al., 2015; Deng and Wang, 2016; Fan et al., 2016). However, D-O-C-S stable isotopic results showed that the ore-forming fluids were mainly derived from the enriched lithospheric mantle (Mao et al., 2008). The coeval lamprophyre dykes in the Jiaodong gold province, in which carbonate minerals are commonly observed (Sun et al., 2001; Guo et al., 2004; Yang et al., 2004; Ma et al., 2016), are characterized by C–O stable isotopic compositions typical of the upper mantle (Sun et al., 2001). Based on a detailed study of fluid inclusions in quartz veins, Fan et al. (2003) showed that the $CO_2$ concentration gradually decreased from the early to late mineralizing stages. Gold in the mantle is controlled by sulfides (Li and Audétat, 2012; Lorand and Luguet, 2016; Jenner, 2017), which can be destabilized under the oxidizing conditions induced by carbonate melts derived from the crustal recycling. This process is thought to release gold- and sulfur-rich fluid. $CO_2$ has the ability to buffer the pH of this fluid at a level where elevated concentrations of gold can be transported (Phillips and Evans, 2004). We therefore suggest that carbonate metasomatism in the lithospheric mantle may have played a crucial part in the activation, transport, enrichment and mineralization of gold in the eastern North China Craton.

## 8. Genesis of carbonate melts

Type 1 carbonate metasomatism is characterized by high $^{87}Sr/^{86}Sr$ ratios of 0.706–0.713 (Figure 6a). The metasomatic agent should be high Ca/Al ratios and $CO_2$ concentrations and low $SiO_2$ and $Al_2O_3$ concentrations, as seen in the carbonate melt formed from the partial melting of carbonated eclogite (Figure 8). The Mesozoic (124 Ma) Laiwu-Zibo carbonatite in the Shandong Province with $^{87}Sr/^{86}Sr$ ratios of 0.7095–0.7106 is thought to have been derived from the partial melting of the South China Block and its accompanying carbonate sediments, which was subducted into the deep lithospheric mantle beneath the eastern North China Craton in the Triassic (Ying et al., 2004). The continental material of the South China Block should have been subducted into the mantle to depths >200 km (Ye et al., 2000). The enriched mantle resulting from crust-mantle interactions during continental deep subduction is suggested to the source of the postcollisional mafic igneous rocks (Zhao et al., 2013). The Triassic (210–201 Ma) and early Cretaceous (133–111 Ma) postcollisional mafic igneous rocks of the Jiaodong Peninsula involve recycled continental crust material and have evolved Sr isotopic compositions ($^{87}Sr/^{86}Sr$=0.706–0.714) (Dai et al., 2016) consistent with the Sr isotopic composition ($^{87}Sr/^{86}Sr$=0.706–0.713) of clinopyroxenes affected by Type 1 carbonate metasomatism (Figure 6a). The late Triassic mafic igneous rocks show high Ca/Al and $(La/Yb)_N$ ratios and low Ti/Eu ratios (Figure 7) typical of carbonate metasomatism. Carbonate sediments were well developed along the northern margin of the South China Block from the Neoproterozoic to the Paleozoic (Zheng and Hu, 2010). Carbonated ultrahigh pressure eclogites also occur widely in the Sulu orogenic belt (Proyer et al., 2013; Liu P L et al., 2015; Chen Y X et al., 2016). We therefore propose that the deep subduction of the South China Block carried significant amounts of carbonate sediments into the lithospheric mantle beneath the North China Craton, inducing intense Type 1 carbonate metasomatism, which provided a prerequisite for the final destruction of the eastern North China Craton.

Combined with the positive relationship between Ca/Al and $CO_2$ and the negative relationship between Ca/Al and $SiO_2$ in the carbonate melt (Figure 8b and c), the low Ca/Al ratio in clinopyroxene affected by Type 2 and Type 3 carbonate metasomatism (Figures 4d, e and 5b, e) implies that their metasomatic agents should have high $SiO_2$ and low $CO_2$ contents. This is consistent with clinopyroxenes of Type 3 carbonate metasomatism, which show the relatively high Ti/Eu ratios (Figure 5c and f) considered to be a result of silicate metasomatism. The low and variable Sr isotopic compositions ($^{87}Sr/^{86}Sr$=0.7022–0.7056) indicate that the carbonate melt of Type 2 and Type 3 metasomatism was mainly derived from the asthenospheric mantle, but also involves recycled crustal material in variable proportions. This is demonstrated by the Changle lherzolite xenoliths, in which high $^{87}Sr/^{86}Sr$ ratio (>0.7035) and low $^{87}Sr/^{86}Sr$ ratio (<0.7024) clinopyroxenes are suggested to record the carbonate metasomatism caused by recycled oceanic crust and upwelling of the asthenospheric mantle, respectively (Deng et al., 2017). The elemental and Mg-Zn stable isotopic compositions show that the Cenozoic basalts from asthenosphere involved a carbonate melt that resulted from crustal recycling in the eastern North China Craton (Zeng et al., 2010; Yang W et al., 2012; Liu et al., 2016; Li et al., 2017). Therefore, Type 2 and Type 3 carbonate metasomatisms are considered as the modifica-

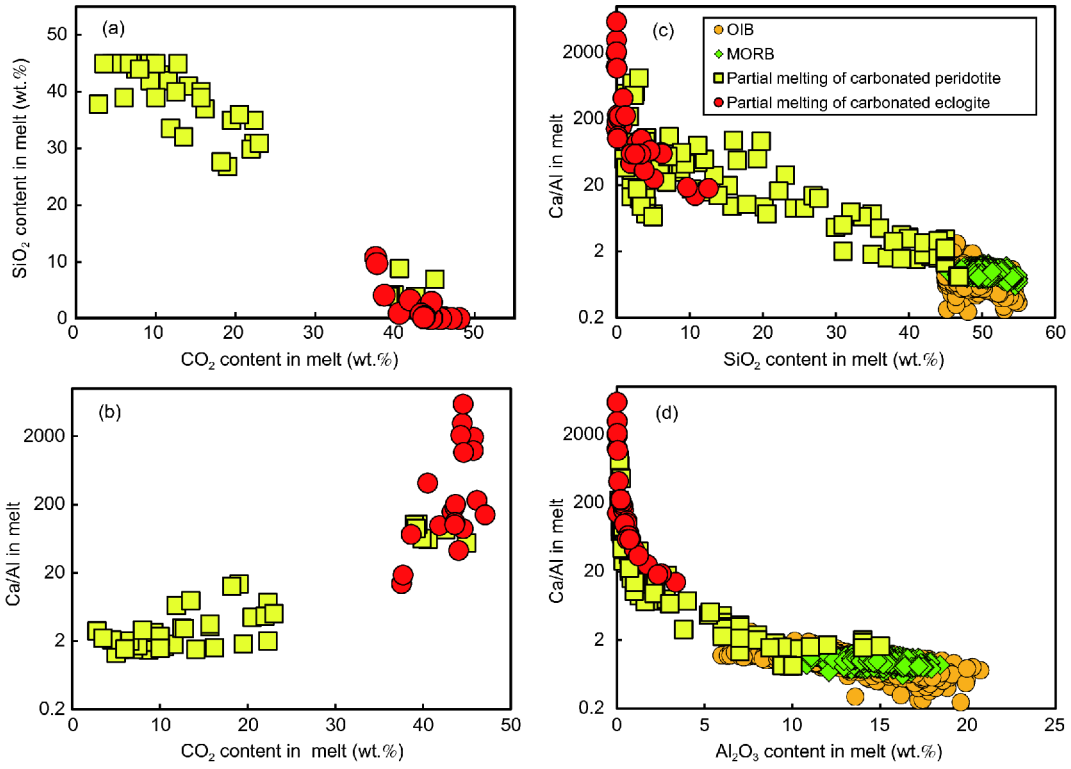


**Figure 8** Variations of ((a), (b)) $CO_2$ with $SiO_2$ and Ca/Al, and ((c), (d)) Ca/Al with $SiO_2$ and $Al_2O_3$ in experimental melts as a result of the parital melting of carbonated eclogite and peridotite. Data for the partial melting of carbonated eclogite are from Dasgupta et al. (2005), Hammouda (2003) and Yaxley and Brey (2004), data for the partial melting of carbonated peridotite are from Dasgupta et al. (2013), Sokol et al. (2016), Brey et al. (2008), Klemme et al. (1995), Gervasoni et al. (2017), Dasgupta et al. (2007), Kruk et al. (2016) and Dalton and Wood (1993); the mid-ocean ridge basalt (MORB) data are from Gale et al. (2013); the oceanic island basalt (OIB) data are from http://georoc.mpch-mainz.gwdg.de/georoc/.

tion of the lithospheric mantle in the eastern North China Craton, which is caused by the carbonate melts derived from the asthenospheric mantle with variable proportions of the recycled crustal material.

## 9. Conclusions

(1) The geochemcial indices of major elements Ca/Al and Mg#, trace elements $(La/Yb)_N$ and Ti/Eu, and the Sr isotopic composition of clinopyroxene in peridotite can be used to trace carbonate metasomatism in the lithospheric mantle.

(2) Three types of carbonate metasomatism were identified in the lithospheric mantle beneath the eastern North China Craton. Type 1 carbonate metasomatism was a result of the interaction between carbonate melt derived from recycled continental crust and the lithospheric mantle before the late Triassic, which is suggested to have provided a prerequisite for the final destruction of the eastern North China Craton. Type 2 and Type 3 carbonate metasomatism that modified the lithospheric mantle in the eastern North China Craton was caused by carbonate melts derived from asthenospheric mantle with variable proportions of recycled crustal material.

(3) The strong carbonate metasomatism of the lithospheric mantle is spatially consistent with the formation of the Jiaodong giant gold deposits, indicating that carbonate metasomatism played a crucial part in the formation of the giant gold province in the eastern North China Craton.

**Acknowledgements** *Three anonymous reviewers are thanked for their detailed and constructive comments. We are grateful for discussions with Dr. Junfeng Zhang, Chao Wang, Wei Chen, Xiaodong Deng, Zaicong Wang, Rong Xu, Jingliang Guo, Zhanke Li and Haijun Xu, which helped to improve this paper. Master student candidates Yang Liu and Luye Zhang and doctoral student candidate Huai Cheng are thanked for their data collection work. This research was co-supported by the National Key R&D Program of China (Grant No. 2016YFC0600103), the National Natural Science Foundation of China (Grant Nos. 41473031, 41530211), the National Program on Key Basic Research Project (Grant No. 2015CB856101) and the MOST Special Fund from the State Key Laboratory of Geological Processes and Mineral Resources, China University of Geosciences (Grant No. MSFGPMR01).*

## References

Aulbach S, Griffin W L, O'Reilly S Y, McCandless T E. 2004. Genesis and evolution of the lithospheric mantle beneath the Buffalo Head Terrane, Alberta (Canada). Lithos, 77: 413–451

Baker M B, Stolper E M. 1994. Determining the composition of high-pressure mantle melts using diamond aggregates. Geochim Cosmochim Acta, 58: 2811–2827

Bernstein S, Kelemen P B, Brooks C K. 1998. Depleted spinel harzburgite xenoliths in Tertiary dykes from East Greenland: Restites from high degree melting. Earth Planet Sci Lett, 154: 221–235

Bizzarro M, Stevenson R K. 2003. Major element composition of the lithospheric mantle under the North Atlantic craton: Evidence from peridotite xenoliths of the Sarfartoq area, southwestern Greenland. Contrib Mineral Petrol, 146: 223–240
Blundy J, Dalton J. 2000. Experimental comparison of trace element partitioning between clinopyroxene and melt in carbonate and silicate systems, and implications for mantle metasomatism. Contrib Mineral Petrol, 139: 356–371
Bodinier J L, Godard M, Heinrich D H, Karl K T. 2003. Orogenic, ophiolitic, and abyssal peridotites. Treatise on Geochemistry. Oxford: Elsevier-Pergamon. 103–170
Boyd F R, Pearson D G, Hoal K O, Hoal B G, Nixon P H, Kingston M J, Mertzman S A. 2004. Garnet lherzolites from Louwrensia, Namibia: Bulk composition and *P*/*T* relations. Lithos, 77: 573–592
Boyd F R, Pokhilenko N P, Pearson D G, Mertzman S A, Sobolev N V, Finger L W. 1997. Composition of the Siberian cratonic mantle: Evidence from Udachnaya peridotite xenoliths. Contrib Mineral Petrol, 128: 228–246
Brey G P, Bulatov V K, Girnis A V, Lahaye Y. 2008. Experimental melting of carbonated peridotite at 6–10 GPa. J Petrol, 49: 797–821
Bruce M C, Niu Y, Harbort T A, Holcombe R J. 2000. Petrological, geochemical and geochronological evidence for a Neoproterozoic ocean basin recorded in the Marlborough terrane of the northern New England Fold Belt. Aust J Earth Sci, 47: 1053–1064
Carlson R W, Pearson D G, James D E. 2005. Physical, chemical, and chronological characteristics of continental mantle. Rev Geophys, 43: RG1001
Carter Hearn Jr B. 2004. The Homestead kimberlite, central Montana, USA: Mineralogy, xenocrysts, and upper-mantle xenoliths. Lithos, 77: 473–491
Chen C F, Liu Y S, Foley S F, Ducea M N, He D T, Hu Z C, Chen W, Zong K Q. 2016. Paleo-Asian oceanic slab under the North China craton revealed by carbonatites derived from subducted limestones. Geology, 44: 1039–1042
Chen C F, Liu Y S, Foley S F, Ducea M N, Geng X L, Zhang W, Xu R, Hu Z C, Zhou L, Wang Z C. 2017. Carbonated sediment recycling and its contribution to lithospheric refertilization under the northern North China Craton. Chem Geol, 466: 641–653
Chen G D. 1956. Examples of “activizing region”in the chinese platform with special reference to the “cathaysia” problem (in Chinese with English abstract). Acta Geol Sin, 36: 239–272
Chen Y X, Tang J, Zheng Y F, Wu Y B. 2016. Geochemical constraints on petrogenesis of marble-hosted eclogites from the Sulu orogen in China. Chem Geol, 436: 35–53
Chu Z Y, Wu F Y, Walker R J, Rudnick R L, Pitcher L, Puchtel I S, Yang Y H, Wilde S A. 2009. Temporal evolution of the lithospheric mantle beneath the eastern North China Craton. J Petrol, 50: 1857–1898
Coltorti M, Bonadiman C, Hinton R W, Siena F, Upton B G J. 1999. Carbonatite metasomatism of the oceanic upper mantle: Evidence from clinopyroxenes and glasses in ultramafic xenoliths of Grande Comore, Indian Ocean. J Petrol, 40: 133–165
Dai L Q, Zheng Y F, Zhao Z F. 2016. Termination time of peak decratonization in North China: Geochemical evidence from mafic igneous rocks. Lithos, 240-243: 327–336
Dalton J A, Wood B J. 1993. The compositions of primary carbonate melts and their evolution through wallrock reaction in the mantle. Earth Planet Sci Lett, 119: 511–525
Dasgupta R, Hirschmann M M, Dellas N. 2005. The effect of bulk composition on the solidus of carbonated eclogite from partial melting experiments at 3 GPa. Contrib Mineral Petrol, 149: 288–305
Dasgupta R, Hirschmann M M, Smith N D. 2007. Partial melting experiments of peridotite+$CO_2$ at 3 GPa and genesis of alkalic ocean island basalts. J Petrol, 48: 2093–2124
Dasgupta R, Mallik A, Tsuno K, Withers A C, Hirth G, Hirschmann M M. 2013. Carbon-dioxide-rich silicate melt in the Earth’s upper mantle. Nature, 493: 211–215
Dawson J B. 2002. Metasomatism and partial melting in upper-mantle peridotite xenoliths from the Lashaine volcano, northern Tanzania. J Petrol, 43: 1749–1777
Deng J, Wang Q. 2016. Gold mineralization in China: Metallogenic provinces, deposit types and tectonic framework. Gondwana Res, 36: 219–274
Deng J F, Mo X X, Zhao H L, Wu Z X, Luo Z H, Su S G. 2004. A new model for the dynamic evolution of Chinese lithosphere: ‘continental roots–plume tectonics’. Earth-Sci Rev, 65: 223–275
Deng L, Liu Y, Zong K, Zhu L, Xu R, Hu Z, Gao S. 2017. Trace element and Sr isotope records of multi-episode carbonatite metasomatism on the eastern margin of the North China Craton. Geochem Geophys Geosyst, 18: 220–237
Dong S, Zhang Y, Zhang F, Cui J, Chen X, Zhang S, Miao L, Li J, Shi W, Li Z, Huang S, Li H. 2015. Late Jurassic-Early Cretaceous continental convergence and intracontinental orogenesis in East Asia: A synthesis of the Yanshan Revolution. J Asian Earth Sci, 114: 750–770
Downes H. 2004. Ultramafic xenoliths from the Bearpaw Mountains, Montana, USA: Evidence for multiple metasomatic events in the lithospheric mantle beneath the Wyoming craton. J Petrol, 45: 1631–1662
Eggins S M, Rudnick R L, McDonough W F. 1998. The composition of peridotites and their minerals: A laser-ablation ICP–MS study. Earth Planet Sci Lett, 154: 53–71
Falloon T J, Green D H, Danyushevsky L V, Faul U H. 1999. Peridotite melting at 1.0 and 1.5 GPa: An experimental evaluation of techniques using diamond aggregates and mineral mixes for determination of near-solidus melts. J Petrol, 40: 1343–1375
Fan H R, Feng K, Li X H, Hu F F, Yang K F. 2016. Mesozoic gold mineralization in the Jiaodong and Korean peninsulas (in Chinese with English abstract). Acta Petrol Sin, 32: 3225–3238
Fan H R, Zhai M G, Xie Y H, Yang J H. 2003. Ore-forming fluids associated with granite-hosted gold mineralization at the Sanshandao deposit, Jiaodong gold province, China. Mineralium Deposita, 38: 739–750
Franz L, Brey G P, Okrusch M. 1996. Steady state geotherm, thermal disturbances, and tectonic development of the lower lithosphere underneath the Gibeon Kimberlite Province, Namibia. Contrib Mineral Petrol, 126: 181–198
Gaetani G A, Grove T L. 1998. The influence of water on melting of mantle peridotite. Contrib Mineral Petrol, 131: 323–346
Gale A, Dalton C A, Langmuir C H, Su Y, Schilling J G. 2013. The mean composition of ocean ridge basalts. Geochem Geophys Geosyst, 14: 489–518
Gao S, Rudnick R L, Carlson R W, McDonough W F, Liu Y S. 2002. Re–Os evidence for replacement of ancient mantle lithosphere beneath the North China craton. Earth Planet Sci Lett, 198: 307–322
Gao S, Rudnick R L, Xu W L, Yuan H L, Liu Y S, Walker R J, Puchtel I S, Liu X, Huang H, Wang X R, Yang J. 2008. Recycling deep cratonic lithosphere and generation of intraplate magmatism in the North China Craton. Earth Planet Sci Lett, 270: 41–53
Gao S, Rudnick R L, Yuan H L, Liu X M, Liu Y S, Xu W L, Ling W L, Ayers J, Wang X C, Wang Q H. 2004. Recycling lower continental crust in the North China craton. Nature, 432: 892–897
Gao S, Zhang J F, Xu W L, Liu Y S. 2009. Delamination and destruction of the North China Craton. Chin Sci Bull, 54: 1962–1973
Gervasoni F, Klemme S, Rohrbach A, Grützner T, Berndt J. 2017. Experimental constraints on mantle metasomatism caused by silicate and carbonate melts. Lithos, 282-283: 173–186
Ghorbani M R, Middlemost E A K. 2000. Geochemistry of pyroxene inclusions from the Warrumbungle Volcano, New South Wales, Australia. Am Miner, 85: 1349–1367
Grassi D, Schmidt M W. 2011. The Melting of Carbonated Pelites from 70 to 700 km Depth. J Petrol, 52: 765–789
Green D H, Wallace M E. 1988. Mantle metasomatism by ephemeral carbonatite melts. Nature, 336: 459–462
Gregoire M. 2003. Garnet lherzolites from the Kaapvaal Craton (South Africa): Trace element evidence for a metasomatic history. J Petrol, 44: 629–657

Gregoire M, Tinguely C, Bell D, Leroex A. 2005. Spinel lherzolite xenoliths from the Premier kimberlite (Kaapvaal craton, South Africa): Nature and evolution of the shallow upper mantle beneath the Bushveld complex. Lithos, 84: 185–205
Griffin W L, Doyle B J, Ryan C G, Pearson N J, Suzanne Y O, Davies R, Kivi K, Van Achterbergh E, Natapov L M. 1999. Layered mantle lithosphere in the Lac de Gras area, Slave craton: Composition, structure and origin. J Petrol, 40: 705–727
Griffin W L, Kaminsky F V, Ryan C G, O'Reilly S Y, Win T T, Ilupin I P. 1996. Thermal state and composition of the lithospheric mantle beneath the Daldyn kimberlite field, Yakutia. Tectonophysics, 262: 19–33
Griffin W L, Natapov L M, O'Reilly S Y, van Achterbergh E, Cherenkova A F, Cherenkov V G. 2005. The Kharamai kimberlite field, Siberia: Modification of the lithospheric mantle by the Siberian Trap event. Lithos, 81: 167–187
Guo F, Fan W, Wang Y, Zhang M. 2004. Origin of early Cretaceous calc-alkaline lamprophyres from the Sulu orogen in eastern China: Implications for enrichment processes beneath continental collisional belt. Lithos, 78: 291–305
Hammouda T. 2003. High-pressure melting of carbonated eclogite and experimental constraints on carbon recycling and storage in the mantle. Earth Planet Sci Lett, 214: 357–368
Hammouda T, Laporte D. 2000. Ultrafast mantle impregnation by carbonatite melts. Geology, 28: 283–285
Hellebrand E, Snow J E. 2003. Deep melting and sodic metasomatism underneath the highly oblique-spreading Lena Trough (Arctic Ocean). Earth Planet Sci Lett, 216: 283–299
Hofmann A W. 1997. Mantle geochemistry: The message from oceanic volcanism. Nature, 385: 219–229
Holm P M, Prægel N O. 2006. Cumulates from primitive rift-related East Greenland Paleogene magmas: Petrological and isotopic evidence from the ultramafic complexes at Kælvegletscher and near Kærven. Lithos, 92: 251–275
Hou T, Zhang Z, Keiding J K, Veksler I V. 2015. Petrogenesis of the ultrapotassic Fanshan intrusion in the North China Craton: Implications for lithospheric mantle metasomatism and the origin of apatite ores. J Petrol, 56: 893–918
Ionov D A. 2004. Chemical variations in peridotite xenoliths from Vitim, Siberia: Inferences for REE and Hf behaviour in the garnet-facies upper mantle. J Petrol, 45: 343–367
Ionov D A, O'Reilly S Y, Genshaft Y S, Kopylova M G. 1996. Carbonate-bearing mantle peridotite xenoliths from Spitsbergen: Phase relationships, mineral compositions and trace-element residence. Contrib Mineral Petrol, 125: 375–392
Ionov D A, Ashchepkov I, Jagoutz E. 2005a. The provenance of fertile off-craton lithospheric mantle: Sr-Nd isotope and chemical composition of garnet and spinel peridotite xenoliths from Vitim, Siberia. Chem Geol, 217: 41–75
Ionov D A, Ashchepkov I V, Stosch H G, Witt-Eickschen G, Seck H A. 1993a. Garnet peridotite xenoliths from the Vitim volcanic field, Baikal region: The nature of the garnet—Spinel peridotite transition zone in the continental mantle. J Petrol, 34: 1141–1175
Ionov D A, Chanefo I, Bodinier J L. 2005b. Origin of Fe-rich lherzolites and wehrlites from Tok, SE Siberia by reactive melt percolation in refractory mantle peridotites. Contrib Mineral Petrol, 150: 335–353
Ionov D A, Chazot G, Chauvel C, Merlet C, Bodinier J L. 2006. Trace element distribution in peridotite xenoliths from Tok, SE Siberian craton: A record of pervasive, multi-stage metasomatism in shallow refractory mantle. Geochim Cosmochim Acta, 70: 1231–1260
Ionov D A, DuPuy C, O'Reilly S Y, Kopylova M G, Genshaft Y S. 1993b. Carbonated peridotite xenoliths from Spitsbergen: Implications for trace element signature of mantle carbonate metasomatism. Earth Planet Sci Lett, 119: 283–297
Ionov D A, Hofmann A W. 1995. NbTa-rich mantle amphiboles and micas: Implications for subduction-related metasomatic trace element fractionations. Earth Planet Sci Lett, 131: 341–356
Ionov D A, Prikhodko V S, Bodinier J L, Sobolev A V, Weis D. 2005c. Lithospheric mantle beneath the south-eastern Siberian craton: Petrology of peridotite xenoliths in basalts from the Tokinsky Stanovik. Contrib Mineral Petrol, 149: 647–665
Jenner F E. 2017. Cumulate causes for the low contents of sulfide-loving elements in the continental crust. Nat Geosci, 10: 524–529
Kamenetsky V S, Yaxley G M. 2015. Carbonate–silicate liquid immiscibility in the mantle propels kimberlite magma ascent. Geochim Cosmochim Acta, 158: 48–56
Kerrick D M, Connolly J A D. 2001. Metamorphic devolatilization of subducted marine sediments and the transport of volatiles into the Earth's mantle.. Nature, 411: 293–296
Kim N, Cheong A C, Yi K, Jeong Y J, Koh S M. 2016. Post-collisional carbonatite-hosted rare earth element mineralization in the Hongcheon area, central Gyeonggi massif, Korea: Ion microprobe monazite U-Th-Pb geochronology and Nd-Sr isotope geochemistry. Ore Geol Rev, 79: 78–87
Klemme S, van der Laan S R, Foley S F, Günther D. 1995. Experimentally determined trace and minor element partitioning between clinopyroxene and carbonatite melt under upper mantle conditions. Earth Planet Sci Lett, 133: 439–448
Kopylova M G, Caro G. 2004. Mantle xenoliths from the southeastern Slave craton: Evidence for chemical zonation in a thick, cold lithosphere. J Petrol, 45: 1045–1067
Kopylova M G, Russell J K, Cookenboo H. 1999. Petrology of peridotite and pyroxenite xenoliths from the Jericho Kimberlite: Implications for the thermal state of the mantle beneath the Slave craton, northern Canada. J Petrol, 40: 79–104
Kruk A N, Sokol A G, Chebotarev D A, Palyanov Y A, Sobolev N V. 2016. Composition of a carbonatitic melt in equilibrium with lherzolite at 5.5–6.3 GPa and 1350°C. Dokl Earth Sci, 467: 303–307
Lee C T, Rudnick R L, McDonough W F, Horn I. 2000. Petrologic and geochemical investigation of carbonates in peridotite xenoliths from northeastern Tanzania. Contrib Mineral Petrol, 139: 470–484
Lee C T A, Luffi P, Chin E J. 2011. Building and destroying continental mantle. Annu Rev Earth Planet Sci, 39: 59–90
Li J W, Bi S J, Selby D, Chen L, Vasconcelos P, Thiede D, Zhou M F, Zhao X F, Li Z K, Qiu H N. 2012. Giant Mesozoic gold provinces related to the destruction of the North China craton. Earth Planet Sci Lett, 349-350: 26–37
Li S G, Yang W, Ke S, Meng X, Tian H C, Xu L J, He Y S, Huang J, Wang X C, Xia Q K, Sun W D, Yang X Y, Ren Z Y, Wei H Q, Liu Y S, Meng F C, Yan J. 2017. Deep carbon cycles constrained by a large-scale mantle Mg isotope anomaly in eastern China. Nat Sci Rev, 4: 111–120
Li Y, Audétat A. 2012. Partitioning of V, Mn, Co, Ni, Cu, Zn, As, Mo, Ag, Sn, Sb, W, Au, Pb, and Bi between sulfide phases and hydrous basanite melt at upper mantle conditions. Earth Planet Sci Lett, 355-356: 327–340
Lin W, Wang J, Liu F, Ji W B, Wang Q C. 2013. Late Mesozoic extension structures on the North China Craton and adjacent regions and its geodynamics (in Chinese with English abstract). Acta Petrol Sin, 29: 1791–1810
Litasov K D, Foley S F, Litasov Y D. 2000. Magmatic modification and metasomatism of the subcontinental mantle beneath the Vitim volcanic field (East Siberia): Evidence from trace element data on pyroxenite and peridotite xenoliths from Miocene picrobasalt. Lithos, 54: 83–114
Liu D Y, Nutman A P, Compston W, Wu J S, Shen Q H. 1992. Remnants of ≥3800 Ma crust in the Chinese part of the Sino-Korean craton. Geology, 20: 339–342
Liu F, Zong K Q, Liu Y S, Hu Z C, Zhu L Y, Xu R. 2015. Methane-bearing melt inclusion in olivine phenocryst in Cenozoic alkaline basalt from Eastern China and its geological significance. Chin Sci Bull, 60: 1310–1319
Liu P L, Wu Y, Chen Y, Zhang J F, Jin Z M. 2015. UHP impure marbles from the Dabie Mountains: Metamorphic evolution and carbon cycling in continental subduction zones. Lithos, 212-215: 280–297
Liu S A, Wang Z Z, Li S G, Huang J, Yang W. 2016. Zinc isotope evidence for a large-scale carbonated mantle beneath eastern China. Earth Planet

Sci Lett, 444: 169–178
Liu Y S, Gao S, Hu Z C, Gao C G, Zong K Q, Wang D B. 2010. Continental and oceanic crust recycling-induced melt-peridotite interactions in the Trans-North China Orogen: U-Pb dating, Hf isotopes and trace elements in zircons from mantle xenoliths. J Petrol, 51: 537–571
Liu Y S, Gao S, Kelemen P B, Xu W L. 2008. Recycled crust controls contrasting source compositions of Mesozoic and Cenozoic basalts in the North China Craton. Geochim Cosmochim Acta, 72: 2349–2376
Liu Y S, Gao S, Lee C T A, Hu S H, Liu X M, Yuan H L. 2005. Melt-peridotite interactions: Links between garnet pyroxenite and high-Mg# signature of continental crust. Earth Planet Sci Lett, 234: 39–57
Liu Y S, He D T, Gao C G, Foley S, Gao S, Hu Z C, Zong K Q, Chen H H. 2015. First direct evidence of sedimentary carbonate recycling in subduction-related xenoliths. Sci Rep, 5: 11547
Lorand J P, Luguet A. 2016. Chalcophile and siderophile elements in mantle rocks: Trace elements controlled by trace minerals. Rev Mineral Geochem, 81: 441–488
Ma L, Jiang S Y, Hofmann A W, Xu Y G, Dai B Z, Hou M L. 2016. Rapid lithospheric thinning of the North China Craton: New evidence from cretaceous mafic dikes in the Jiaodong Peninsula. Chem Geol, 432: 1–15
Machetel P, Humler E. 2003. High mantle temperature during Cretaceous avalanche. Earth Planet Sci Lett, 208: 125–133
MacKenzie J M, Canil D. 1999. Composition and thermal evolution of cratonic mantle beneath the central Archean Slave Province, NWT, Canada. Contrib Mineral Petrol, 134: 313–324
Malarkey J, Wittig N, Graham Pearson D, Davidson J P. 2011. Characterising modal metasomatic processes in young continental lithospheric mantle: A microsampling isotopic and trace element study on xenoliths from the Middle Atlas Mountains, Morocco. Contrib Mineral Petrol, 162: 289–302
Mao J, Wang Y, Li H, Pirajno F, Zhang C, Wang R. 2008. The relationship of mantle-derived fluids to gold metallogenesis in the Jiaodong Peninsula: Evidence from D-O-C-S isotope systematics. Ore Geol Rev, 33: 361–381
McCammon C, Kopylova M G. 2004. A redox profile of the Slave mantle and oxygen fugacity control in the cratonic mantle. Contrib Mineral Petrol, 148: 55–68
Meng Q R. 2003. What drove late Mesozoic extension of the northern China-Mongolia tract? Tectonophysics, 369: 155–174
Menzies A, Westerlund K, Grütter H, Gurney J, Carlson J, Fung A, Nowicki T. 2004. Peridotitic mantle xenoliths from kimberlites on the Ekati Diamond Mine property, N.W.T., Canada: Major element compositions and implications for the lithosphere beneath the central Slave craton. Lithos, 77: 395–412
Menzies M A, Fan W, Zhang M. 1993. Palaeozoic and Cenozoic lithoprobes and the loss of >120 km of Archaean lithosphere, Sino-Korean craton, China. Geol Soc London Spec Publ, 76: 71–81
Molina J F, Poli S. 2000. Carbonate stability and fluid composition in subducted oceanic crust: An experimental study on $H_2O$-$CO_2$-bearing basalts. Earth Planet Sci Lett, 176: 295–310
Neumann E R, Wulff-Pedersen E, Pearson N J, Spencer E A. 2002. Mantle xenoliths from Tenerife (Canary Islands): Evidence for reactions between mantle peridotites and silicic carbonatite melts inducing Ca metasomatism. J Petrol, 43: 825–857
Niu X, Chen B, Liu A, Suzuki K, Ma X. 2012. Petrological and Sr-Nd-Os isotopic constraints on the origin of the Fanshan ultrapotassic complex from the North China Craton. Lithos, 149: 146–158
Niu X L, Chen B, Feng G Y, Liu F, Yang J S. 2017. Origin of lamprophyres from the northern margin of the North China Craton: Implications for mantle metasomatism. J Geological Soc, 174: 353–364
Niu Y L. 2005. Generation and evolution of basaltic magmas: Some basic concepts and a new view on the origin of Mesozoic-Cenozoic basaltic volcanism in eastern China. Geol J China Univ, 11: 9–46
Pearson D G, Canil D, Shirey S B, Heinrich D H, Karl K T. 2003. Treatise on Geochemistry. Oxford: Elsevier-Pergamon. 171–275
Peslier A H. 2002. The lithospheric mantle beneath continental margins: Melting and melt-rock reaction in Canadian Cordillera xenoliths. J Petrol, 43: 2013–2047
Phillips G N, Evans K A. 2004. Role of $CO_2$ in the formation of gold deposits. Nature, 429: 860–863
Pickering-Witter J, Johnston A D. 2000. The effects of variable bulk composition on the melting systematics of fertile peridotitic assemblages. Contrib Mineral Petrol, 140: 190–211
Powell W, Zhang M, O'Reilly S Y, Tiepolo M. 2004. Mantle amphibole trace-element and isotopic signatures trace multiple metasomatic episodes in lithospheric mantle, western Victoria, Australia. Lithos, 75: 141–171
Proyer A, Rolfo F, Zhu Y F, Castelli D, Compagnoni R. 2013. Ultrahigh-pressure metamorphism in the magnesite+aragonite stability field: Evidence from two impure marbles from the Dabie-Sulu UHPM belt. J Metamorph Geol, 31: 35–48
Rapp R P, Shimizu N, Norman M D, Applegate G S. 1999. Reaction between slab-derived melts and peridotite in the mantle wedge: Experimental constraints at 3.8 GPa. Chem Geol, 160: 335–356
Roach I C. 2004. Mineralogy, textures and *P-T* relationships of a suite of xenoliths from the Monaro Volcanic Province, New South Wales, Australia. J Petrol, 45: 739–758
Rudnick R L, McDonough W F, Chappell B W. 1993. Carbonatite metasomatism in the northern Tanzanian mantle: Petrographic and geochemical characteristics. Earth Planet Sci Lett, 114: 463–475
Russell J K, Porritt L A, Lavallée Y, Dingwell D B. 2012. Kimberlite ascent by assimilation-fuelled buoyancy. Nature, 481: 352–356
Saltzer R L. 2001. The spatial distribution of garnets and pyroxenes in mantle peridotites: Pressure-temperature history of peridotites from the Kaapvaal Craton. J Petrol, 42: 2215–2229
Schmidberger S S, Francis D. 1999. Nature of the mantle roots beneath the North American craton: Mantle xenolith evidence from Somerset Island kimberlites. Lithos, 48: 195–216
Schmidberger S S, Francis D. 2001. Constraints on the trace element composition of the Archean mantle root beneath Somerset Island, Arctic Canada. J Petrol, 42: 1095–1117
Schmidberger S S, Simonetti A, Francis D. 2003. Small-scale Sr isotope investigation of clinopyroxenes from peridotite xenoliths by laser ablation MC-ICP-MS—Implications for mantle metasomatism. Chem Geol, 199: 317–329
Schwab B E, Johnston A D. 2001. Melting systematics of modally variable, compositionally intermediate peridotites and the effects of mineral fertility. J Petrol, 42: 1789–1811
Sharygin V V, Golovin A V, Pokhilenko N P, Kamenetsky V S. 2007. Djerfisherite in the Udachnaya-East pipe kimberlites (Sakha-Yakutia, Russia): Paragenesis, composition and origin. Eur J Mineral, 19: 51–63
Shi L, Francis D, Ludden J, Frederiksen A, Bostock M. 1998. Xenolith evidence for lithospheric melting above anomalously hot mantle under the northern Canadian Cordillera. Contrib Mineral Petrol, 131: 39–53
Simon N S C, Irvine G J, Davies G R, Pearson D G, Carlson R W. 2003. The origin of garnet and clinopyroxene in "depleted" Kaapvaal peridotites. Lithos, 71: 289–322
Sleep N H. 2003. Survival of Archean cratonal lithosphere. J Geophys Res, 108: 2302
Sleep N H. 2005. Evolution of the continental lithosphere. Annu Rev Earth Planet Sci, 33: 369–393
Sokol A G, Kruk A N, Chebotarev D A, Palyanov Y N. 2016. Carbonatite melt-peridotite interaction at 5.5–7.0 GPa: Implications for metasomatism in lithospheric mantle. Lithos, 248-251: 66–79
Stiefenhofer J, Viljoen K S, Marsh J S. 1997. Petrology and geochemistry of peridotite xenoliths from the Letlhakane kimberlites, Botswana. Contrib Mineral Petrol, 127: 147–158
Su B, Chen Y, Guo S, Chu Z Y, Liu J B, Gao Y J. 2016. Carbonatitic metasomatism in orogenic dunites from Lijiatun in the Sulu UHP terrane, eastern China. Lithos, 262: 266–284
Sun J G, Hu S X, Shen K, Yao F L. 2001. Research on C, O isotopic geochemistry of intermediate-basic and intermediate-acid dykes in goldfields of Jiaodong Peninsula (in Chinese with English abstract).

Acta Petrol Mineral, 20: 47–56
Sun J, Liu C Z, Wu F Y, Yang Y H, Chu Z Y. 2012. Metasomatic origin of clinopyroxene in Archean mantle xenoliths from Hebi, North China Craton: Trace-element and Sr-isotope constraints. Chem Geol, 328: 123–136
Sun W D, Ding X, Hu Y H, Li X H. 2007. The golden transformation of the Cretaceous plate subduction in the west Pacific. Earth Planet Sci Lett, 262: 533–542
Tong X R, Liu Y S, Hu Z C, Chen H H, Zhou L, Hu Q H, Xu R, Deng L X, Chen C F, Yang L, Gao S. 2016. Accurate determination of Sr isotopic compositions in clinopyroxene and silicate glasses by LA-MC-ICP-MS. Geostand Geoanal Res, 40: 85–99
van Achterbergh E, Griffin W L, Ryan C G, O'Reilly S Y, Pearson N J, Kivi K, Doyle B J. 2004. Melt inclusions from the deep Slave lithosphere: Implications for the origin and evolution of mantle-derived carbonatite and kimberlite. Lithos, 76: 461–474
Varela M E, Clocchiatti R, Kurat G, Schiano P. 1999. Silicic glasses in hydrous and anhydrous mantle xenoliths from Western Victoria, Australia: At least two different sources. Chem Geol, 153: 151–169
Wallace M E, Green D H. 1988. An experimental determination of primary carbonatite magma composition. Nature, 335: 343–346
Walter M J. 1998. Melting of garnet peridotite and the origin of komatiite and depleted lithosphere. J Petrol, 39: 29–60
Wang C G, Liang Y, Xu W L, Dygert N. 2013. Effect of melt composition on basalt and peridotite interaction: Laboratory dissolution experiments with applications to mineral compositional variations in mantle xenoliths from the North China Craton. Contrib Mineral Petrol, 166: 1469–1488
Wang C, Jin Z M, Gao S, Zhang J F, Zheng S. 2010. Eclogite-melt/peridotite reaction: Experimental constrains on the destruction mechanism of the North China Craton. Sci China Earth Sci, 40: 541–555
Wang C Y, Liu Y S, Min N, Zong K Q, Hu Z C, Gao S. 2016. Paleo-Asian oceanic subduction-related modification of the lithospheric mantle under the North China Craton: Evidence from peridotite xenoliths in the Datong basalts. Lithos, 261: 109–127
Wang C, Liu Y, Zhang J, Jin Z. 2016. Carbonate melt form subduction zone: The key for craton destruction. Goldschmidt Abstracts, 3307
Wang Y J, Fan W M, Zhang G W, Zhang Y H. 2013. Phanerozoic tectonics of the South China Block: Key observations and controversies. Gondwana Res, 23: 1273–1305
Wang Z S, Kusky T M, Capitanio F A. 2016. Lithosphere thinning induced by slab penetration into a hydrous mantle transition zone. Geophys Res Lett, 43: 11,567–11,577
Wasylenki L E, Baker M B, Kent A J R, Stolper E M. 2003. Near-solidus melting of the shallow upper mantle: Partial melting experiments on depleted peridotite. J Petrol, 44: 1163–1191
Whitehead K, Le Roex A, Class C, Bell D. 2002. Composition and Cretaceous thermal structure of the upper mantle beneath the Damara Mobile Belt: Evidence from nephelinite-hosted peridotite xenoliths, Swakopmund, Namibia. J Geological Soc, 159: 307–321
Windley B F, Maruyama S, Xiao W J. 2010. Delamination/thinning of subcontinental lithospheric mantle under Eastern China: The role of water and multiple subduction. Am J Sci, 310: 1250–1293
Woodland A B, Seitz H M, Yaxley G M. 2004. Varying behaviour of Li in metasomatised spinel peridotite xenoliths from western Victoria, Australia. Lithos, 75: 55–66
Wu D, Liu Y S, Chen C F, Xu R, Ducea M N, Hu Z C, Zong K Q. 2017. *In-situ* trace element and Sr isotopic compositions of mantle xenoliths constrain two-stage metasomatism beneath the northern North China Craton. Lithos, 288-289: 338–351
Wu F Y, Lin J Q, Wilde S A, Zhang X, Yang J H. 2005. Nature and significance of the Early Cretaceous giant igneous event in eastern China. Earth Planet Sci Lett, 233: 103–119
Wu F Y, Walker R J, Yang Y H, Yuan H L, Yang J H. 2006. The chemical-temporal evolution of lithospheric mantle underlying the North China Craton. Geochim Cosmochim Acta, 70: 5013–5034
Xia Q K, Hao Y, Li P, Deloule E, Coltorti M, Dallai L, Yang X, Feng M. 2010. Low water content of the Cenozoic lithospheric mantle beneath the eastern part of the North China Craton. J Geophys Res, 115: B07207
Xia Q K, Liu J, Liu S C, Kovács I, Feng M, Dang L. 2013. High water content in Mesozoic primitive basalts of the North China Craton and implications on the destruction of cratonic mantle lithosphere. Earth Planet Sci Lett, 361: 85–97
Xiao Y, Zhang H F, Fan W M, Ying J F, Zhang J, Zhao X M, Su B X. 2010. Evolution of lithospheric mantle beneath the Tan-Lu fault zone, eastern North China Craton: Evidence from petrology and geochemistry of peridotite xenoliths. Lithos, 117: 229–246
Xu R, Liu Y S, Tong X R, Hu Z C, Zong K Q, Gao S. 2013a. In-situ trace elements and Li and Sr isotopes in peridotite xenoliths from Kuandian, North China Craton: Insights into Pacific slab subduction-related mantle modification. Chem Geol, 354: 107–123
Xu R, Liu Y S, Zong K Q, Zou D Y, Deng L X, Tong X R, Hu Z C, Gao S. 2013b. Micro-geochemistry of peridotite xenoliths from Kuandian: Implications for evolution of lithospheric mantle (in Chinese with English abstract). Acta Petrol Mineral, 32: 613–636
Xu W L, Hergt J M, Gao S, Pei F P, Wang W, Yang D B. 2008. Interaction of adakitic melt-peridotite: Implications for the high-Mg# signature of Mesozoic adakitic rocks in the eastern North China Craton. Earth Planet Sci Lett, 265: 123–137
Xu W L, Zhou Q J, Pei F P, Yang D B, Gao S, Li Q L, Yang Y H. 2013. Destruction of the North China Craton: Delamination or thermal/chemical erosion? Mineral chemistry and oxygen isotope insights from websterite xenoliths. Gondwana Res, 23: 119–129
Xu X S, O'Reilly S Y, Griffin W L, Zhou X M, Huang X L. 1998. The nature of the Cenozoic lithosphere at Nushan, eastern China: Mantle Dynamics and Plate Interactions in Eastern Asia, Geodynamics 27, American Geophysical Union. 167–195
Xu X S, O'Reilly S Y, Griffin W L, Zhou X M. 2000. Genesis of young lithospheric mantle in southeastern China: An LAM-ICPMS trace element study. J Petrol, 41: 111–148
Xu Y G, Huang X L, Thirlwall M F, Chen X M. 2003a. "Reactive" harzburgite xenoliths from Huinan, Jilin province and their implications for deep dynamic processes (in Chinese with English abstract). Acta Petrol Sin, 19: 19–26
Xu Y G, Menzies M A, Thirlwall M F, Huang X L, Liu Y, Chen X M. 2003b. "Reactive" harzburgites from Huinan, NE China: Products of the lithosphere-asthenosphere interaction during lithospheric thinning? Geochim Cosmochim Acta, 67: 487–505
Xu Y G. 2001. Thermo-tectonic destruction of the archaean lithospheric keel beneath the sino-korean craton in china: Evidence, timing and mechanism. Phys Chem Earth Part A-Solid Earth Geodesy, 26: 747–757
Yan G H, Mu B L, Xu B L, He G Q, Han B F, Wang S G, Tong Y, Ren K X, Yang B, Hong D W, Qiao G S, Xu R H, Zhang R H, Chu Z Y. 2002. Characteristics and implications of Nd, Sr and Pb isotopes and chronology of Phanerozoic alkaline-rich intrusions in North China (in Chinese with English abstract). Geol Rev, 48: 69–76
Yan G H, Mu B L, Zeng Y S, Cai J H, Ren K X, Li F T. 2007. Igneous carbonatites in North China Craton: The temporal and spatial distribution, Sr and Nd isotopic charateristics and their geological significance (in Chinese with English abstract). Geol J China Univ, 13: 463–473
Yan G H, Tan L K, Xu B L, Mou B L, Shao H X, Chen T L, Tong Y, Ren K X, Yang B. 2001. Petrogeochemical characteristics of Indosinian alkaline intrusions in Yinshan Area (in Chinese with English abstract). Acta Petrol Mineral, 20: 281–292
Yang J H, Chung S L, Zhai M G, Zhou X H. 2004. Geochemical and Sr-Nd-Pb isotopic compositions of mafic dikes from the Jiaodong Peninsula, China: Evidence for vein-plus-peridotite melting in the lithospheric mantle. Lithos, 73: 145–160
Yang J H, Wu F Y, Wilde S A. 2003. A review of the geodynamic setting of large-scale Late Mesozoic gold mineralization in the North China Craton: An association with lithospheric thinning. Ore Geol Rev, 23: 125–152

Yang J H, Sun J F, Zhang M, Wu F Y, Wilde S A. 2012. Petrogenesis of silica-saturated and silica-undersaturated syenites in the northern North China Craton related to post-collisional and intraplate extension. Chem Geol, 328: 149–167
Yang J H, O'Reilly S, Walker R J, Griffin W, Wu F Y, Zhang M, Pearson N. 2010. Diachronous decratonization of the Sino-Korean craton: Geochemistry of mantle xenoliths from North Korea. Geology, 38: 799–802
Yang J J, Jahn B M. 2000. Deep subduction of mantle-derived garnet peridotites from the Su-Lu UHP metamorphic terrane in China. J Metamorph Geol, 18: 167–180
Yang W, Teng F Z, Zhang H F, Li S G. 2012. Magnesium isotopic systematics of continental basalts from the North China craton: Implications for tracing subducted carbonate in the mantle. Chem Geol, 328: 185–194
Yaxley G M, Kamenetsky V, Green D H, Falloon T J. 1997. Glasses in mantle xenoliths from western Victoria, Australia, and their relevance to mantle processes. Earth Planet Sci Lett, 148: 433–446
Yaxley G M, Brey G P. 2004. Phase relations of carbonate-bearing eclogite assemblages from 2.5 to 5.5 GPa: Implications for petrogenesis of carbonatites. Contrib Mineral Petrol, 146: 606–619
Yaxley G M, Crawford A J, Green D H. 1991. Evidence for carbonatite metasomatism in spinel peridotite xenoliths from western Victoria, Australia. Earth Planet Sci Lett, 107: 305–317
Yaxley G M, Green D H. 1994. Experimental demonstration of refractory carbonate-bearing eclogite and siliceous melt in the subduction regime. Earth Planet Sci Lett, 128: 313–325
Yaxley G M, Green D H. 1998. Reactions between eclogite and peridotite: Mantle refertilisation by subduction of oceanic crust. Schweiz Mineral Petrogr Mitt, 78: 243–255
Yaxley G M, Green D H, Kamenetsky V. 1998. Carbonatite metasomatism in the southeastern Australian lithosphere. J Petrol, 39: 1917–1930
Yaxley G M, Kamenetsky V. 1999. *In situ* origin for glass in mantle xenoliths from southeastern Australia: Insights from trace element compositions of glasses and metasomatic phases. Earth Planet Sci Lett, 172: 97–109
Ye K, Cong B L, Ye D N. 2000. The possible subduction of continental material to depths greater than 200 km. Nature, 407: 734–736
Yin A. 2010. Cenozoic tectonic evolution of Asia: A preliminary synthesis. Tectonophysics, 488: 293–325
Ying J, Zhou X, Zhang H. 2004. Geochemical and isotopic investigation of the Laiwu-Zibo carbonatites from western Shandong Province, China, and implications for their petrogenesis and enriched mantle source. Lithos, 75: 413–426
Ying J F, Zhang H F, Kita N, Morishita Y, Shimoda G. 2006. Nature and evolution of Late Cretaceous lithospheric mantle beneath the eastern North China Craton: Constraints from petrology and geochemistry of peridotitic xenoliths from Jünan, Shandong Province, China. Earth Planet Sci Lett, 244: 622–638
Yuan H L, Gao S, Rudnick R L, Jin Z M, Liu Y S, Puchtel I S, Walker R J, Yu R D. 2007. Re-Os evidence for the age and origin of peridotites from the Dabie-Sulu ultrahigh pressure metamorphic belt, China. Chem Geol, 236: 323–338
Zeng G, Chen L H, Xu X S, Jiang S Y, Hofmann A W. 2010. Carbonated mantle sources for Cenozoic intra-plate alkaline basalts in Shandong, North China. Chem Geol, 273: 35–45
Zhang H F. 2009. Peridotite-melt interaction: A key point for the destruction of cratonic lithospheric mantle. Chin Sci Bull, 54: 2008–2026
Zhang H F, Goldstein S L, Zhou X H, Sun M, Zheng J P, Cai Y. 2008. Evolution of subcontinental lithospheric mantle beneath eastern China: Re-Os isotopic evidence from mantle xenoliths in Paleozoic kimberlites and Mesozoic basalts. Contrib Mineral Petrol, 155: 271–293
Zhang H, Liu Y, Hu Z, Zong K, Chen H, Chen C. 2017. Low-$\delta^{13}$C carbonates in the Miocene basalt of the northern margin of the North China Craton: Implications for deep carbon recycling. J Asian Earth Sci, 144: 110–125
Zhang H F. 2005. Transformation of lithospheric mantle through peridotite-melt reaction: A case of Sino-Korean craton. Earth Planet Sci Lett, 237: 768–780
Zhang H F, Sun M, Zhou X H, Zhou M F, Fan W M, Zheng J P. 2003. Secular evolution of the lithosphere beneath the eastern North China Craton: Evidence from Mesozoic basalts and high-Mg andesites. Geochim Cosmochim Acta, 67: 4373–4387
Zhang J F, Wang C, Wang Y F. 2012. Experimental constraints on the destruction mechanism of the North China Craton. Lithos, 149: 91–99
Zhang J, Zhang H F, Kita N, Shimoda G, Morishita Y C, Ying J F, Tang Y J. 2011. Secular evolution of the lithospheric mantle beneath the eastern North China craton: Evidence from peridotitic xenoliths from Late Cretaceous mafic rocks in the Jiaodong region, east-central China. Int Geol Rev, 53: 182–211
Zhang R Y, Pan Y M, Yang Y H, Li T F, Liou J G, Yang J S. 2008. Chemical composition and ultrahigh-*P* metamorphism of garnet peridotites from the Sulu UHP terrane, China: Investigation of major, trace elements and Hf isotopes of minerals. Chem Geol, 255: 250–264
Zhang S H, Zhao Y, Davis G A, Ye H, Wu F. 2014. Temporal and spatial variations of Mesozoic magmatism and deformation in the North China Craton: Implications for lithospheric thinning and decratonization. Earth-Sci Rev, 131: 49–87
Zhang S H, Zhao Y, Ye H, Hou K J, Li C F. 2012. Early Mesozoic alkaline complexes in the northern North China Craton: Implications for cratonic lithospheric destruction. Lithos, 155: 1–18
Zhang Z M, Dong X, Liou J G, Liu F, Wang W, Yui F. 2011. Metasomatism of garnet peridotite from Jiangzhuang, southern Sulu UHP belt: Constraints on the interactions between crust and mantle rocks during subduction of continental lithosphere. J Metamorph Geol, 29: 917–937
Zhao G C, Wilde S A, Cawood P A, Sun M. 2001. Archean blocks and their boundaries in the North China Craton: Lithological, geochemical, structural and P-T path constraints and tectonic evolution. Precambrian Res, 107: 45–73
Zhao G C, Zhai M G. 2013. Lithotectonic elements of Precambrian basement in the North China Craton: Review and tectonic implications. Gondwana Res, 23: 1207–1240
Zhao Z F, Dai L Q, Zheng Y F. 2013. Postcollisional mafic igneous rocks record crust-mantle interaction during continental deep subduction. Sci Rep, 3: 3413
Zheng H R, Hu Z Q. 2010. Atlas of Pre-Mesozoic tectonic lithofacies paleogeography in China (in Chinese). Beijing: Geological Publishing House
Zheng J P. 2009. Comparison of mantle-derived matierals from different spatiotemporal settings: Implications for destructive and accretional processes of the North China Craton. Chin Sci Bull, 54: 1990–2007
Zheng J P, Griffin W L, O'Reilly S Y, Yang J, Li T F, Zhang M, Zhang R Y, Liou J G. 2006. Mineral chemistry of peridotites from Paleozoic, Mesozoic and Cenozoic lithosphere: Constraints on mantle evolution beneath eastern China. J Petrol, 47: 2233–2256
Zheng J P, Griffin W L, O'Reilly S Y, Yu C M, Zhang H F, Pearson N, Zhang M. 2007. Mechanism and timing of lithospheric modification and replacement beneath the eastern North China Craton: Peridotitic xenoliths from the 100 Ma Fuxin basalts and a regional synthesis. Geochim Cosmochim Acta, 71: 5203–5225
Zheng J P, O'Reilly S Y, Griffin W L, Lu F X, Zhang M. 1998. Nature and evolution of Cenozoic lithospheric mantle beneath Shandong peninsula, Sino-Korean craton, eastern China. Int Geol Rev, 40: 471–499
Zheng J P, O'Reilly S Y, Griffin W L, Lu F X, Zhang M, Pearson N J. 2001. Relict refractory mantle beneath the eastern North China block: Significance for lithosphere evolution. Lithos, 57: 43–66
Zheng J P, Sun M, Zhou M F, Robinson P. 2005a. Trace elemental and PGE geochemical constraints of Mesozoic and Cenozoic peridotitic xenoliths on lithospheric evolution of the North China Craton. Geochim Cosmochim Acta, 69: 3401–3418
Zheng J P, Zhang R Y, Griffin W L, Liou J G, O'Reilly S Y. 2005b. Heterogeneous and metasomatized mantle recorded by trace elements in minerals of the Donghai garnet peridotites, Sulu UHP terrane, China. Chem Geol, 221: 243–259

Zheng Y F, Xu Z, Zhao Z F, Dai L Q. 2018. Mesozoic mafic magmatism in North China: Implications for thinning and destruction of cratonic lithosphere. Sci China Earth Sci, 61: 353–385, https://doi.org/10.1007/s11430-017-9160-3

Zhou Q J, Xu W L, Yang D B, Pei F P, Wang W, Yuan H L, Gao S. 2013. Modification of the lithospheric mantle by melt derived from recycled continental crust evidenced by wehrlite xenoliths in Early Cretaceous high-Mg diorites from western Shandong, China. Sci China Earth Sci, 43: 1179–1194

Zhu G, Chen Y, Jiang D, Lin S. 2015. Rapid change from compression to extension in the North China Craton during the Early Cretaceous: Evidence from the Yunmengshan metamorphic core complex. Tectonophysics, 656: 91–110

Zhu G, Jiang D, Zhang B, Chen Y. 2012. Destruction of the eastern North China Craton in a backarc setting: Evidence from crustal deformation kinematics. Gondwana Res, 22: 86–103

Zhu R X, Chen L, Wu F Y, Liu J L. 2011. Timing, scale and mechanism of the destruction of the North China Craton. Sci China Earth Sci, 41: 583–592

Zhu R X, Fan H R, Li J W, Meng Q R, Li S R, Zeng Q D. 2015. Decratonic gold deposits. Sci China Earth Sci, 45: 1153–1168

Zhu R X, Xu Y G, Zhu G, Zhang H F, Xia Q K, Zheng T Y. 2012a. Destruction of the North China Craton. Sci China Earth Sci, 42: 1135–1159

Zhu R X, Yang J H, Wu F Y. 2012b. Timing of destruction of the North China Craton. Lithos, 149: 51–60

Zhu Y S, Yang J H, Sun J F, Wang H. 2017. Zircon Hf-O isotope evidence for recycled oceanic and continental crust in the sources of alkaline rocks. Geology, 45: 407–410

(Responsible editor: Yongfei ZHENG)